Electronic Supplementary Material (ESI) for Green Chemistry.

Supporting Information for

Accessing Secondary Amine Containing Fine Chemicals and Polymers with an Earth-Abundant Hydroaminoalkylation Catalyst

*Manfred Manßen[§], Sabrina S. Scott[§], Danfeng Deng, Cameron H. M. Zheng, Laurel L. Schafer**

[§] These authors contributed equally.

Department of Chemistry, University of British Columbia, Vancouver, British Columbia V6T 1Z4, Canada

Contact: Prof. Laurel L. Schafer (schafer@chem.ubc.ca)

Table of Contents

S1. General Information

All reactions were performed under a N_2 atmosphere using Schlenk or glovebox techniques, unless otherwise stated. All chemicals without a detailed synthesis description here were purchased from commercial sources and used without further purification, unless otherwise noted. Vinyl terminated polypropylene (VTPP) samples were gifted to the Schafer research group by ExxonMobil and were used as received, unless otherwise stated. All amines and alkenes were dried over CaH_2, distilled, and degassed prior to use in catalytic experiments. Solvents were dried according to standard procedures and stored over activated molecular sieves (4 Å). Toluene-d_8 was dried over sodium/ketyl and distilled prior to use. Experiments conducted on an NMR tube scale were performed in J. Young NMR spectroscopy tubes (8" x 5 mm) sealed with PTFE screw caps. All glassware was dried in a 180 °C oven overnight before use.

NMR Spectroscopy. ^{1}H and $^{13}C\{^{1}H\}$ NMR spectra were recorded on Bruker 300 MHz and 400 MHz Avance spectrometers at ambient temperature. Chemical shifts (δ) are given relative to residual protons of the solvent and are reported in parts per million (ppm). Coupling constants J are given in Hertz (Hz). The following abbreviations are used to indicate signal multiplicity: s = singlet, d = doublet, t = triplet, q = quartet, m = multiplet, and br = broad.

Mass Spectrometry. High resolution mass-spectra (HRMS) were measured by the mass spectrometry services at University of British Columbia on a Kratos MS-50 spectrometer using a Bruker maXis Ultra-High Resolution tandem Time-of-Flight (UHR-Qq-ToF) mass spectrometer using a positive electrospray ionization source. Fragment signals are given in mass per charge number (m/z). Gas chromatography/mas-spectra (GC/MS) analyses were conducted on an Agilent 7890B GC with an Agilent 5977 inert chemical ionization (CI) mass detector, utilizing methane as the ionization gas. Field desorption mass spectra (FDMS) were collected using a Jeol AccuTOF-GCv 4G spectrometer equipped with a Field Desorption/Ionization (FD/FI) ion source. The samples were dissolved in dichloromethane (DCM) and were loaded to a FD probe then introduced into the ion source of GC-ToF MS. Mass spectra were acquired in positive mode and fragments are given in mass per charge number (m/z).

X-Ray Diffraction. Single-crystal X-ray structure determination was performed on an APEX II diffractometer at the Department of Chemistry, University of British Columbia.

Differential Scanning Calorimetry. Thermal properties of the samples were measured on a Netzsch DSC Polyma 214 differential scanning calorimeter calibrated using indium. Analyses were performed with a constant flow of N_2 gas at a rate of 60 mL/min with samples of approximately 10-15 mg in a pierced lid aluminum pan. ATPP samples were cooled to -150 °C at a rate of 10 °C/min for two cycles and heated to 30 °C at a rate of 10 °C/min for three cycles with an isothermal hold for 5 minutes at the upper and lower temperature limits between cycles. The glass transition temperatures were determined from the second heating cycle of these measurements. All DSC thermograms are reported with the exotherm in the negative direction.

Thermogravimetric Analysis. Thermal decomposition results were monitored using a Netzsch TG 209 ***F1 Libra***® thermogravimetric analyzer at a heating rate of 10 °C/min from 30 °C to 600 °C with a purge and protective flow of N_2 at a rate of 20 mL/min and 10 mL/min, respectively. The 5%, 50%, and 95% mass loss values were reported for each sample.

IR Spectroscopy. Spectra were recorded at room temperature on a Perkin Elmer FT-IR equipped with an ATR accessory for direct measurement on oils and polymeric materials.

S2. Synthesis and Characterization of Compounds

S2.1 Ligands

3-(2,6-diisopropylphenyl)-1-methyl-1-(1-phenylethyl)urea (L1)

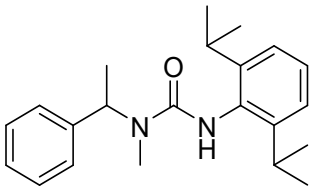

L1 was prepared following a modified literature procedure.[1] 2,6-Diisopropylaniline (14 mL, 13.16 g, 0.074 mol) was dissolved in DCM and the solution was cooled to 0 °C. Triphosgene (7.3146 g, 0.0246 mol) was added in portions as a solid. The solution was stirred for thirty minutes after which *N*,*N*-diisopropylethylamine (DIPEA) (26 mL, 19.292 g, 0.149 mol) was added dropwise and the cold bath removed. The solution was stirred for three h and then *N*-methyl-1-phenylethan-1-amine (10.00 g, 0.074 mol) and a second portion of DIPEA (13 mL, 9.646 g, 0.0746 mol) was added. The solution was stirred for an additional three hours, and then diluted with 80 mL 1M HCl. The organic phase was washed three times with 80 mL 1M HCl and dried over $MgSO_4$, filtered, and concentrated by rotary evaporation to give the crude product. Recrystallization from a concentrated ethyl acetate solution of provided the product as a white solid (21.969 g, 0.0650 mol, 88%).

^{1}H NMR ($CDCl_3$, 400 MHz, rt): δ = 1.31 (s, 12 H, CH-(C*H*$_3$)$_2$), 1.72 (m, 3 H, CH-C*H*$_3$), 3.00 (s, 3 H, N-C*H*$_3$), 3.22-3.12 (m, 2 H, C*H*-(CH$_3$)$_2$), 5.78-5.72 (m, 2 H, C*H*-CH$_3$, N*H*), 7.28 (m, 1 H, Ar-C*H*), 7.37-7.35 (m, 1 H, Ar-C*H*), 7.45-7.39 (m, 2 H, Ar-C*H*), 7.51-7.50 (m, 4 H, Ar-C*H*) ppm.

^{13}C NMR ($CDCl_3$, 101 MHz, rt): δ = 17.34 (*C*H-CH$_3$), 23.81 (CH-(*C*H$_3$)$_2$), 28.79 (*C*H-(CH$_3$)$_2$), 29.82 (N-*C*H$_3$), 52.99 (N-*C*H), 123.36, 126.95, 127.41, 127.63, 128.73, 132.80, 142.12, 146.52 (Ar-*C*, Ar-*C*H), 157.22 (*C*=O) ppm.

HRMS (ESI): m/z calc. for $C_{22}H_{31}N_2O$ [M+H$^+$]: 339.2437. Found: 339.2444.

EA: calc. for $C_{22}H_{30}N_2O$: C, 78.06; H, 8.93; N, 8.28. Found: C, 78.18; H, 8.96; N, 8.31.

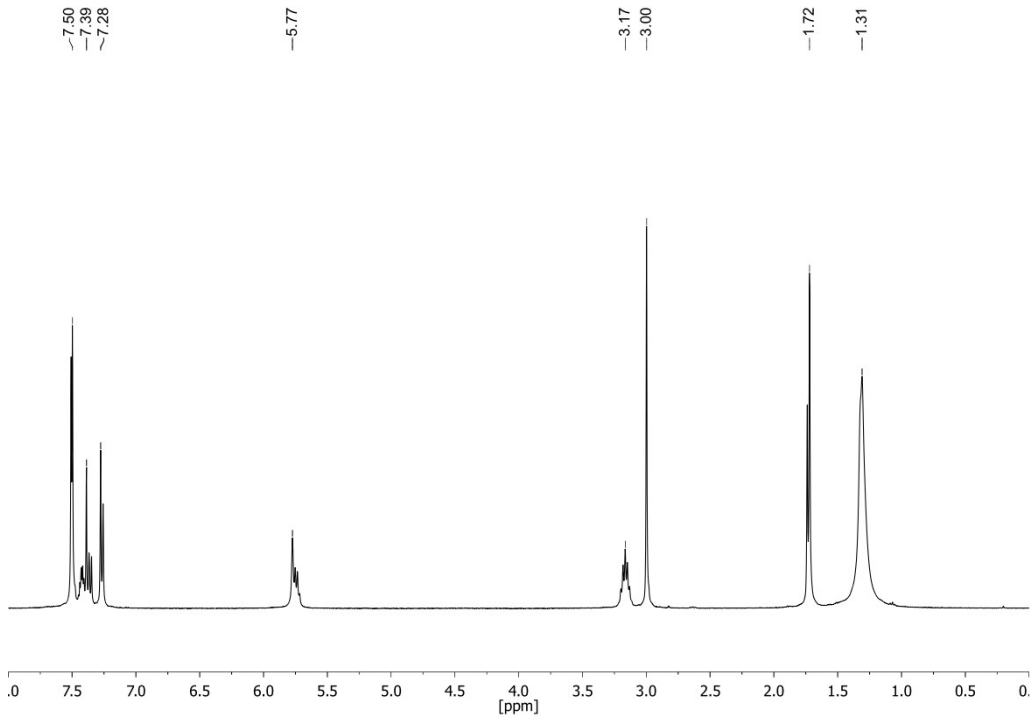

Figure S1. ^{1}H NMR spectrum (400 MHz, $CDCl_3$, rt) of **L1**.

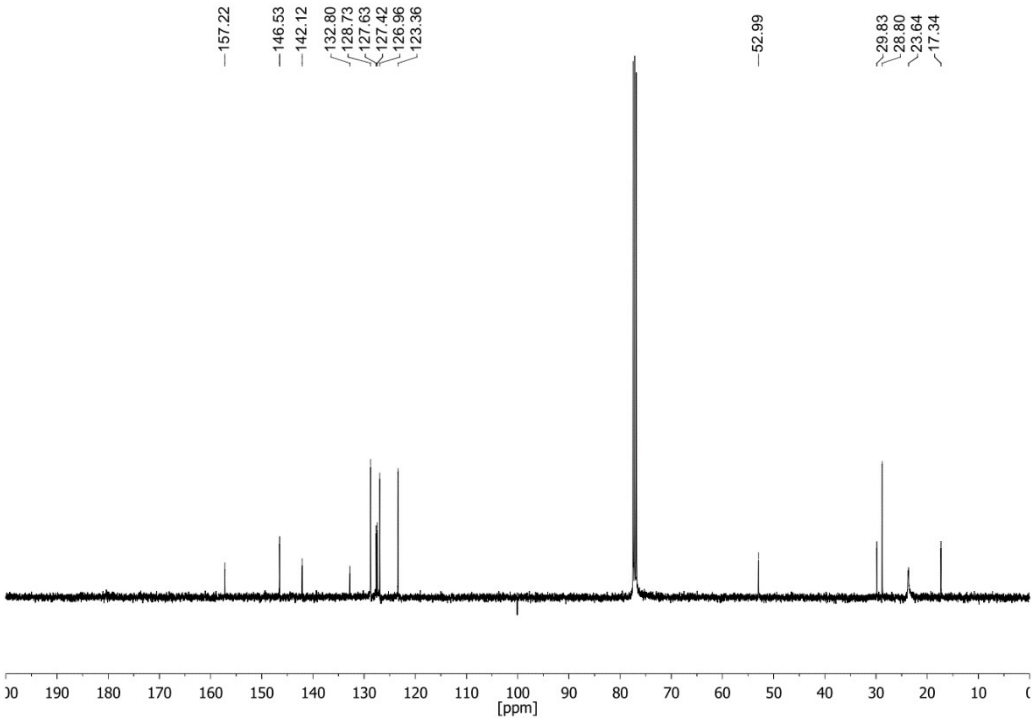

Figure S2. ^{13}C NMR spectrum (101 MHz, $CDCl_3$, rt) of **L1**.

S3. Hydroaminoalkylation Reactions

S3.1 Data Summary of the Small Molecule Scope

General procedure: **L1** (8.5 mg, 0.025 mmol/17.0 mg, 0.05 mmol) was weighed into a vial and dissolved with toluene-d_8 (0.3 mL). $Ti(NMe_2)_4$ (5.6 mg, 0.025 mmol/11.2 mg, 0.05 mmol) was added with a micropipette. The selected amine (0.5 mmol), alkene (0.5 mmol) and 1,3,5-trimethoxybenzene (28.0 mg, 0.166 mmol) were weighed into a different vial, dissolved with toluene-d_8 (0.2 mL) and added to the catalyst system with a micropipette. The resultant reaction mixture was transferred into a J. Young NMR spectroscopy tube and the vials were rinsed with an additional 0.2 mL of toluene-d_8. An initial ^{1}H NMR spectrum was recorded, and the sample was added to a preheated oil bath. All yields were determined by ^{1}H NMR spectroscopy using 1,3,5-trimethoxybenzene as internal standard by integrating of characteristic signals of the starting amine vs. the signal of the internal standard at the start of the reaction and comparing this value with the signal of the amine product vs. the internal standard at the selected time. The selectivity was determined by GC-MS analysis (product area highlighted, *vide infra*).

Table S1. Alkene Scope

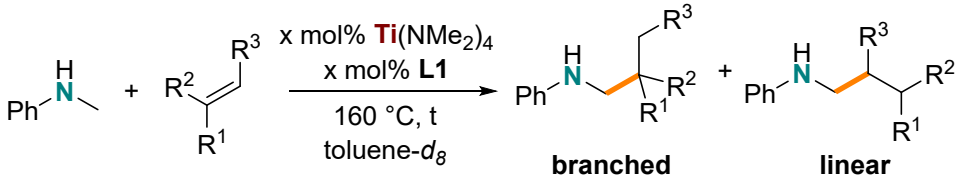

Entry	Alkene	Major Product	Catalyst Loading, Time	Yield (b+l)	Selectivity (a/b)
1		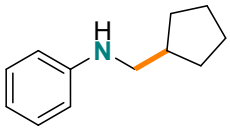	10% 48 h	99%	-
2		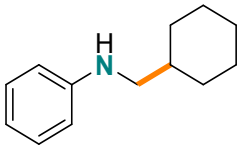	15% 48 h (180 °C)	80%	-
3	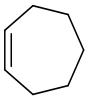	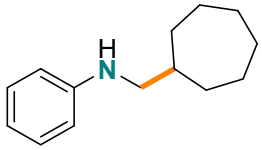	10% 48 h	91%	-
4	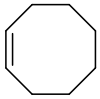	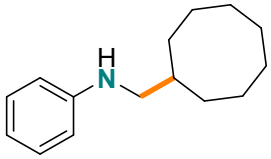	10% 48 h	78%	-
5	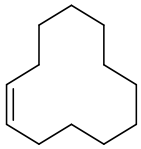	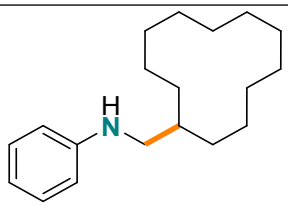	30% 48 h (180 °C)	28%	-

6	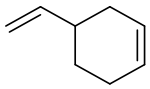	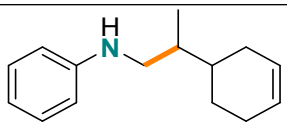	5% 8 h	97%	>99:1
7	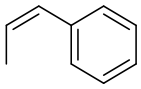	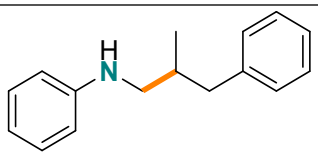	10% 48 h	82%	>99:1
8	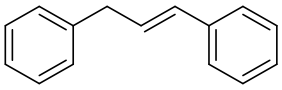	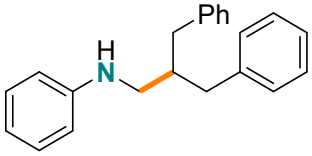	10% 48 h	52%	>99:1
9	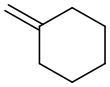	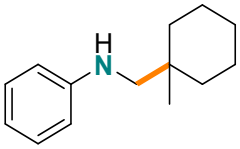	10% 24 h	93%	>99:1

[a] Reaction conditions: Amine (0.5 mmol), alkene (0.5 mmol), toluene-d_8 (0.7 mL), 1,3,5-trimethoxybenzene (0.17 mmol), catalyst loadings as shown. Yields determined by ^{1}H NMR spectroscopy and GC analysis. Selectivity was determined by GC analysis. All data presented have been collected in duplicate or triplicate to ensure consistency of results.

Table S2. Amine Scope

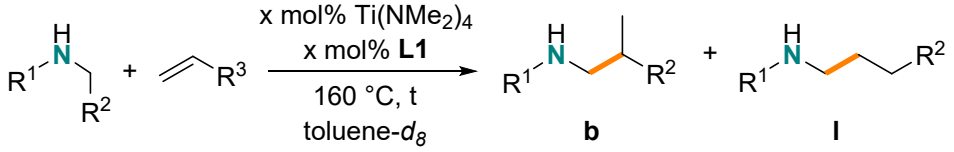

Entry	Amine	Alkene	Catalyst Loading, Time	Yield (b+l)	Selectivity (b/l)
10	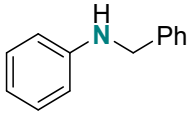	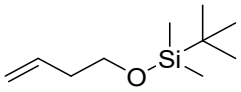	10% 48 h	72%	64:36
11	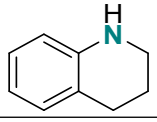	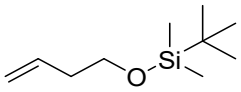	10% 24 h	87%	10:1
12	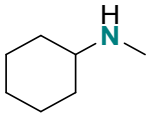	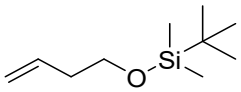	15% 24 h	99%	94:6
13	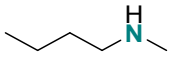	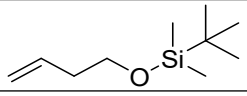	10% 48 h	82%	>99:1

[a] Reaction conditions: Amine (0.5 mmol), alkene (0.5 mmol), toluene-d_8 (0.7 mL), 1,3,5-trimethoxybenzene (0.17 mmol), catalyst loadings as shown. Yields determined by ^{1}H NMR spectroscopy and GC analysis. Selectivity was determined by GC analysis. All data presented have been collected in duplicate or triplicate to ensure consistency of results.

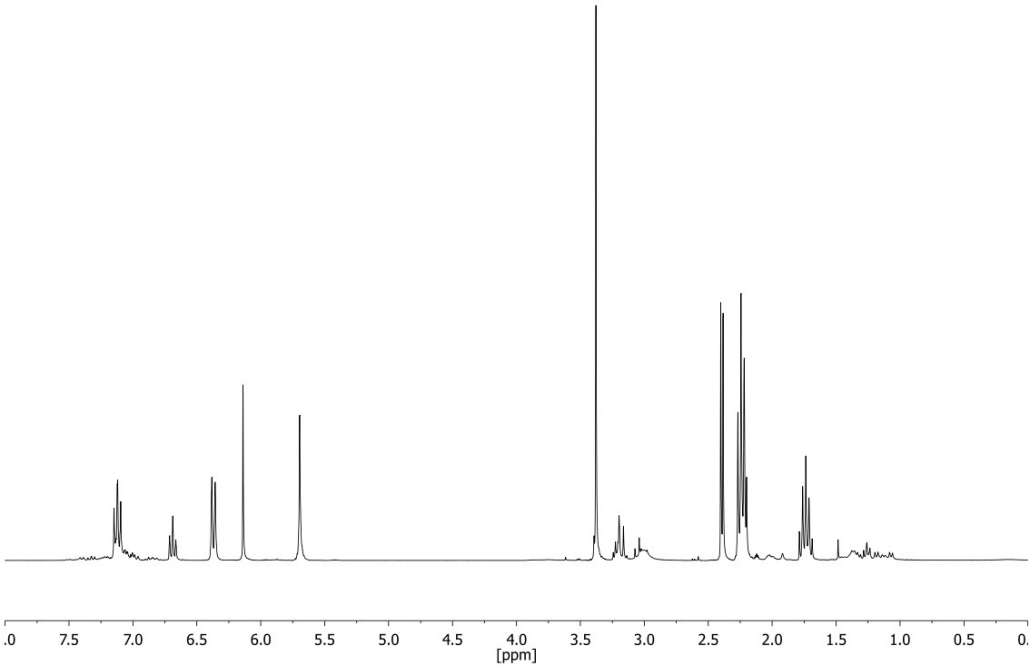

Figure S3. Exemplary t=0 h ^{1}H NMR spectrum (300 MHz, toluene-d_8, rt) of **Entry 1**.

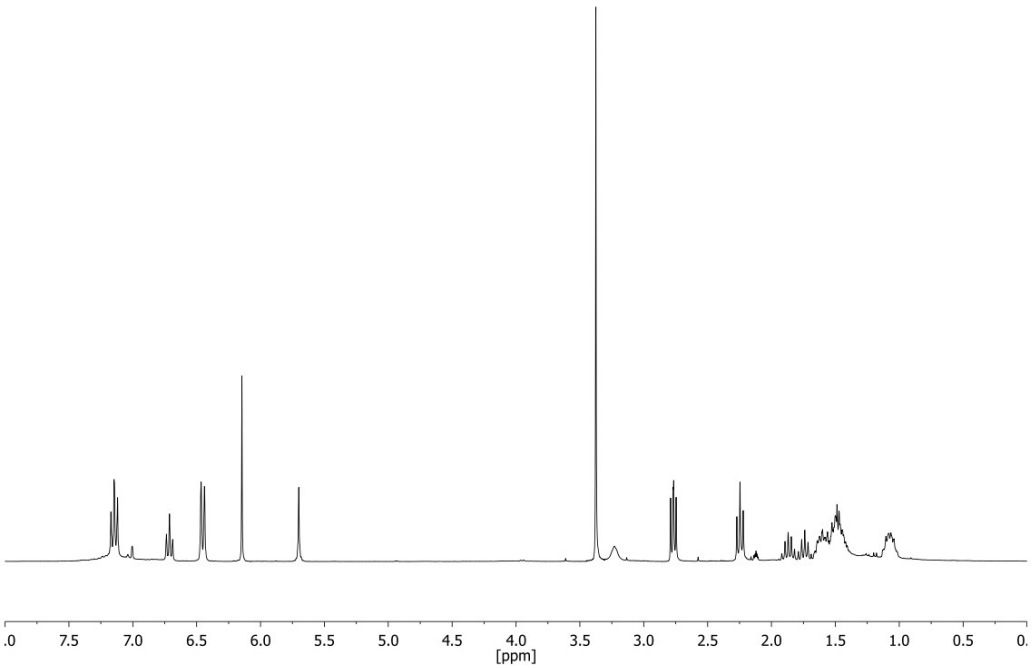

Figure S4. ^{1}H NMR spectrum (300 MHz, toluene-d_8, rt) of **Entry 1**.

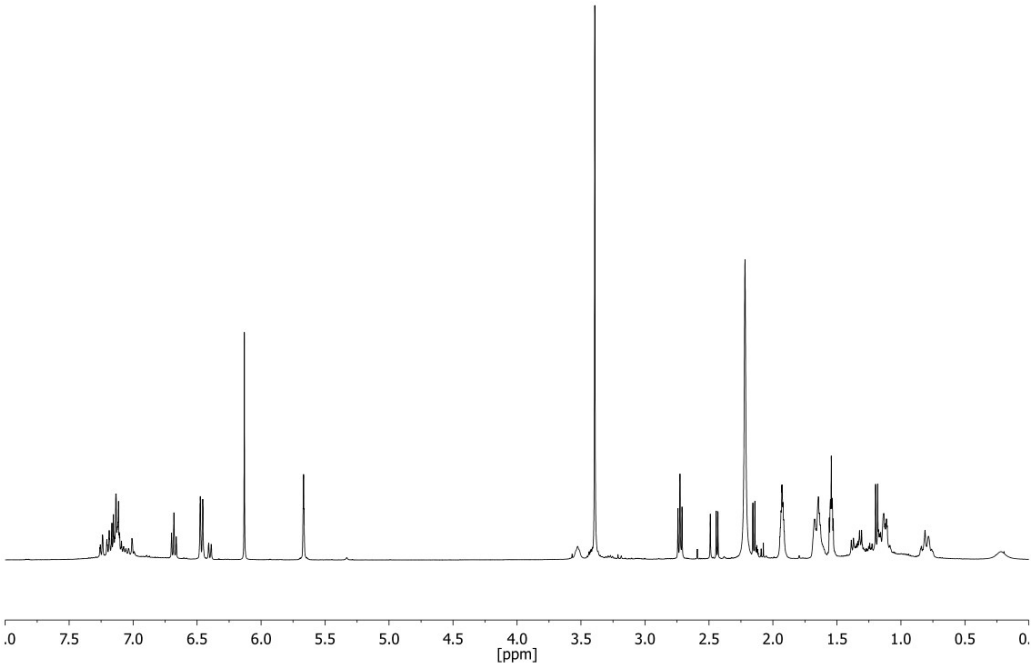

Figure S5. ^{1}H NMR spectrum (300 MHz, toluene-d_8, rt) of **Entry 2**.

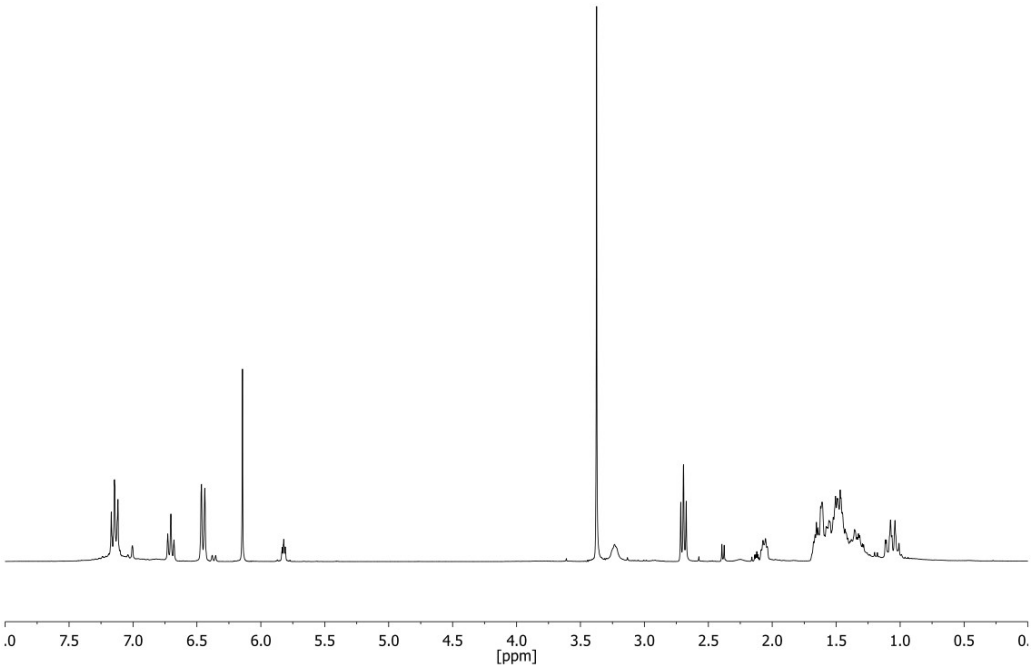

Figure S6. ^{1}H NMR spectrum (300 MHz, toluene-d_8, rt) of **Entry 3**.

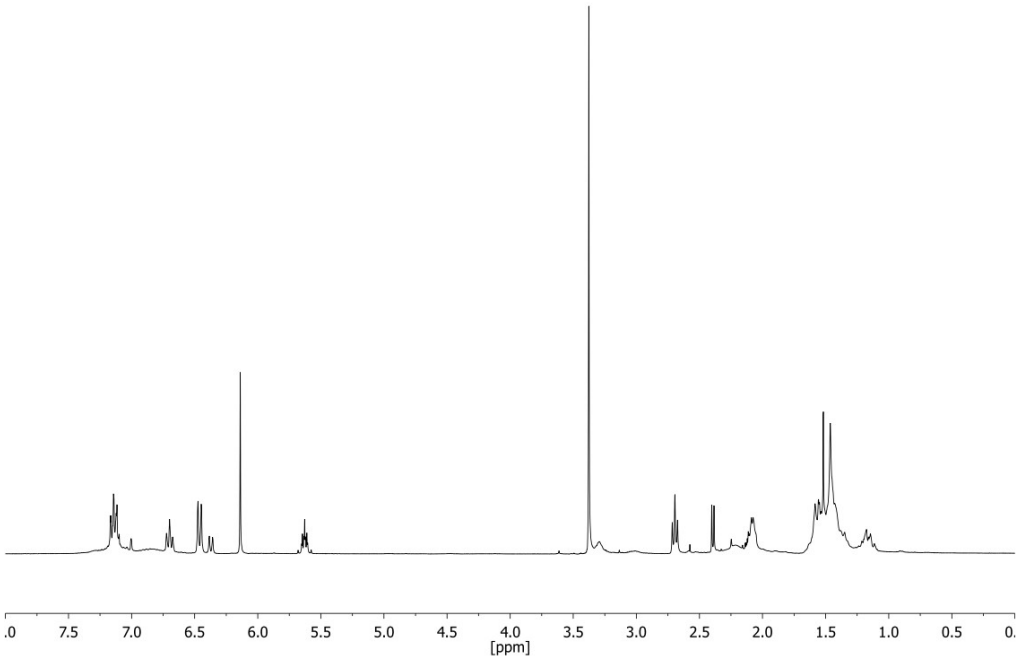

Figure S7. ^{1}H NMR spectrum (300 MHz, toluene-d_8, rt) of **Entry 4**.

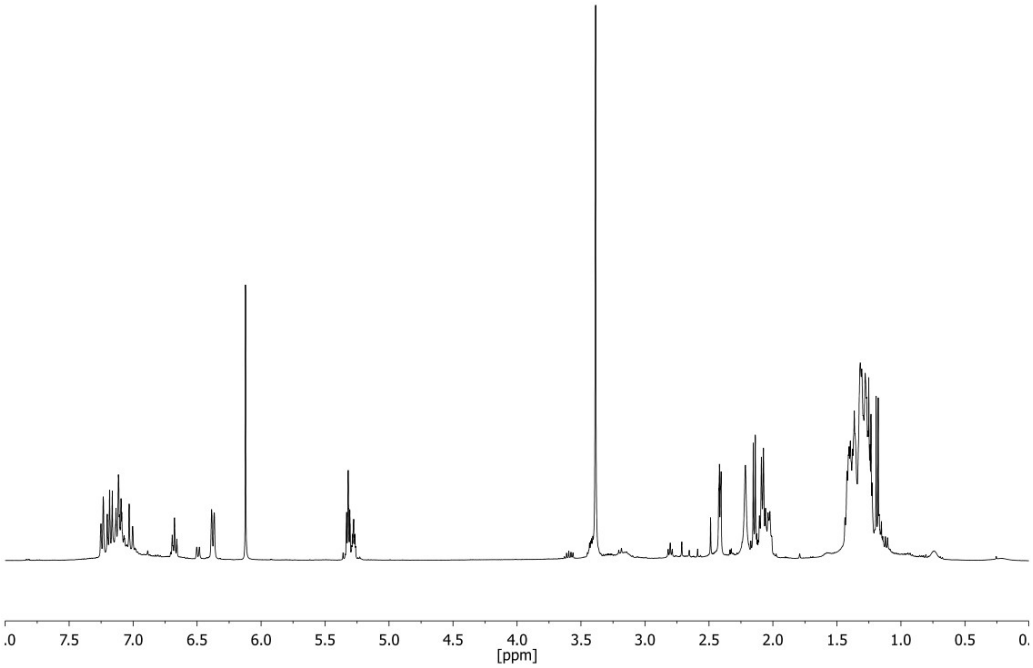

Figure S8. ^{1}H NMR spectrum (300 MHz, toluene-d_8, rt) of **Entry 5**.

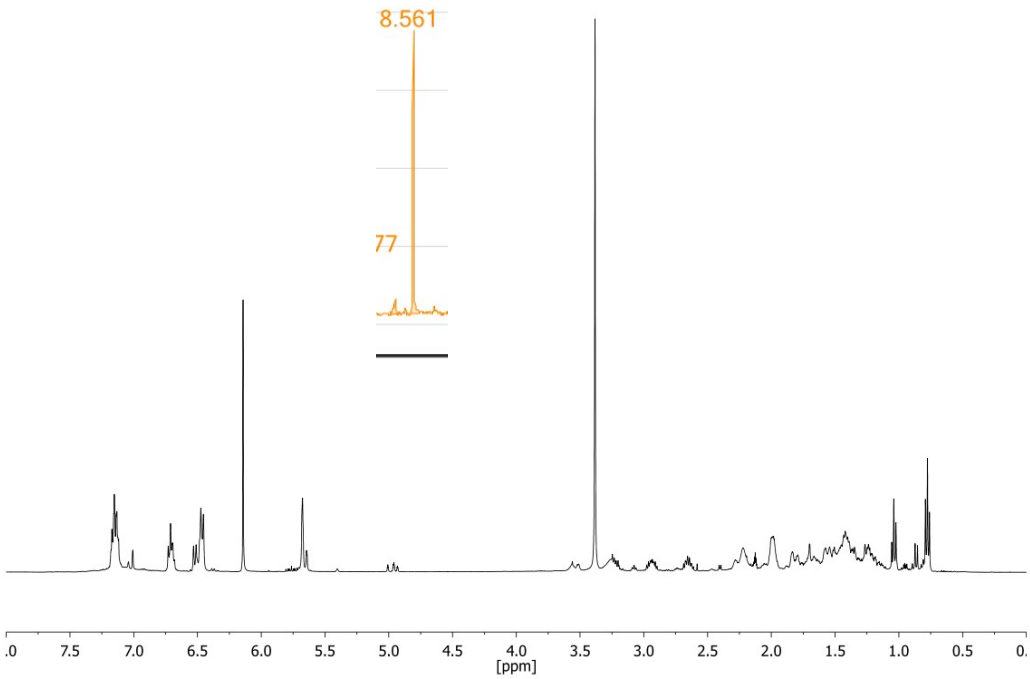

Figure S9. ^{1}H NMR spectrum (300 MHz, toluene-d_8, rt) and branched/linear selectivity via GC of **Entry 6**.

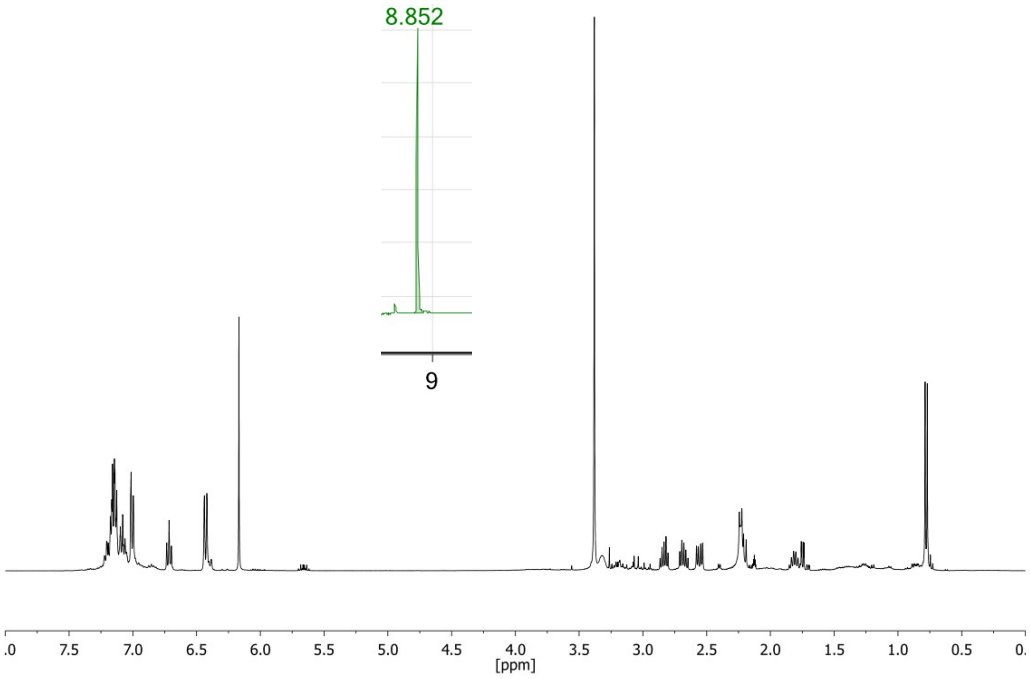

Figure S10. ^{1}H NMR spectrum (300 MHz, toluene-d_8, rt) and branched/linear selectivity via GC of **Entry 7**.

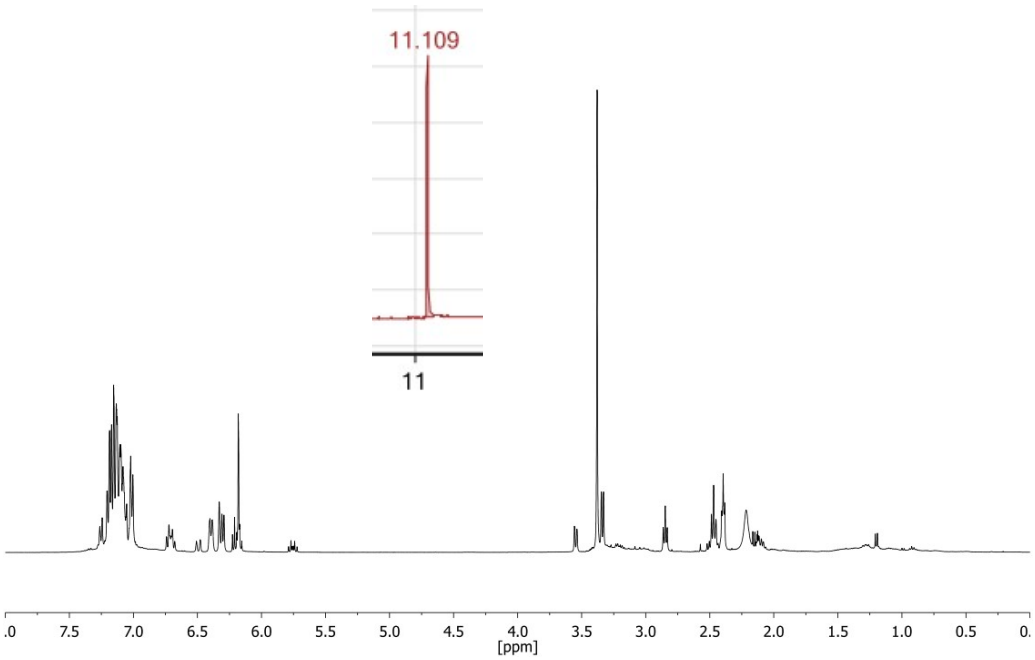

Figure S11. ^{1}H NMR spectrum (300 MHz, toluene-d_8, rt) and branched/linear selectivity via GC of **Entry 8**.

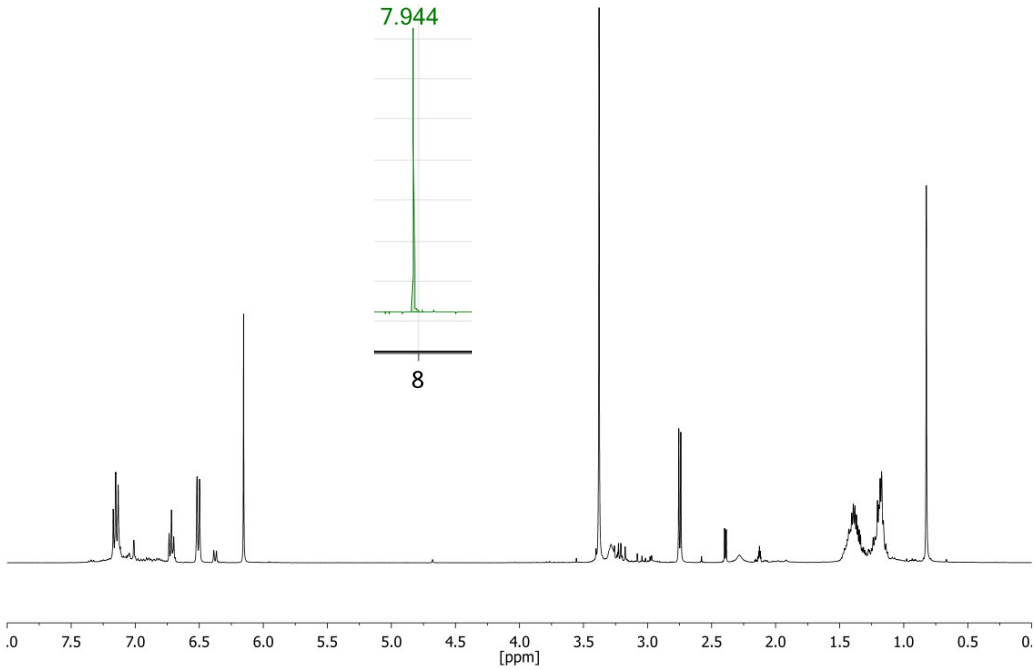

Figure S12. ^{1}H NMR spectrum (300 MHz, toluene-d_8, rt) and branched/linear selectivity via GC of **Entry 9**.

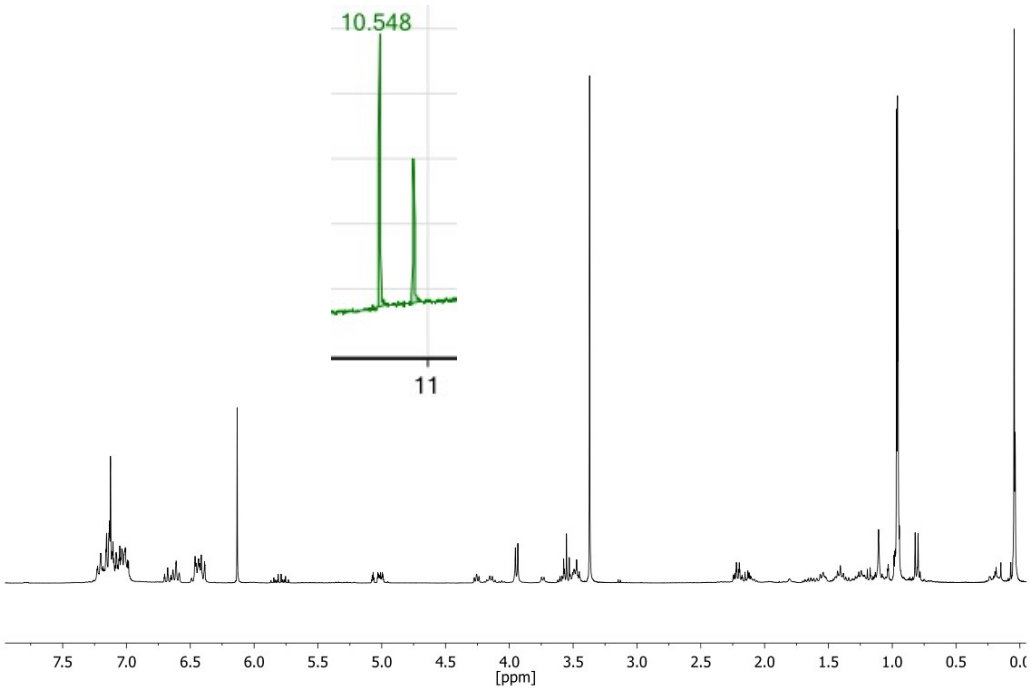

Figure S13. ^{1}H NMR spectrum (300 MHz, toluene-d_8, rt) and branched/linear selectivity via GC of **Entry 10**.

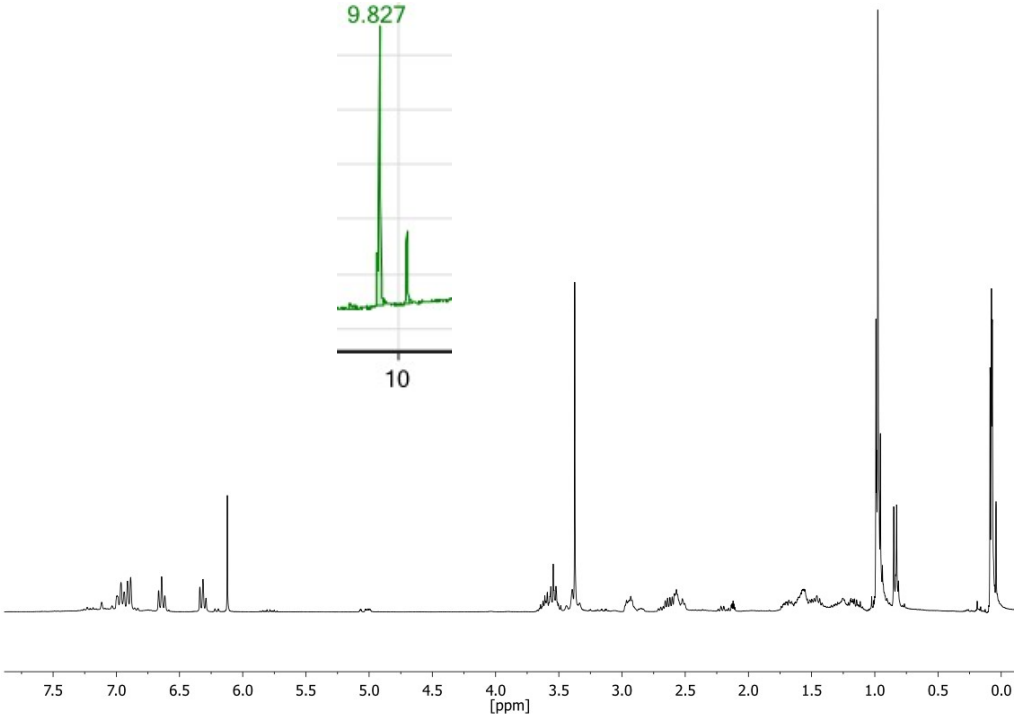

Figure S14. ^{1}H NMR spectrum (300 MHz, toluene-d_8, rt) and branched/linear selectivity via GC of **Entry 11**.

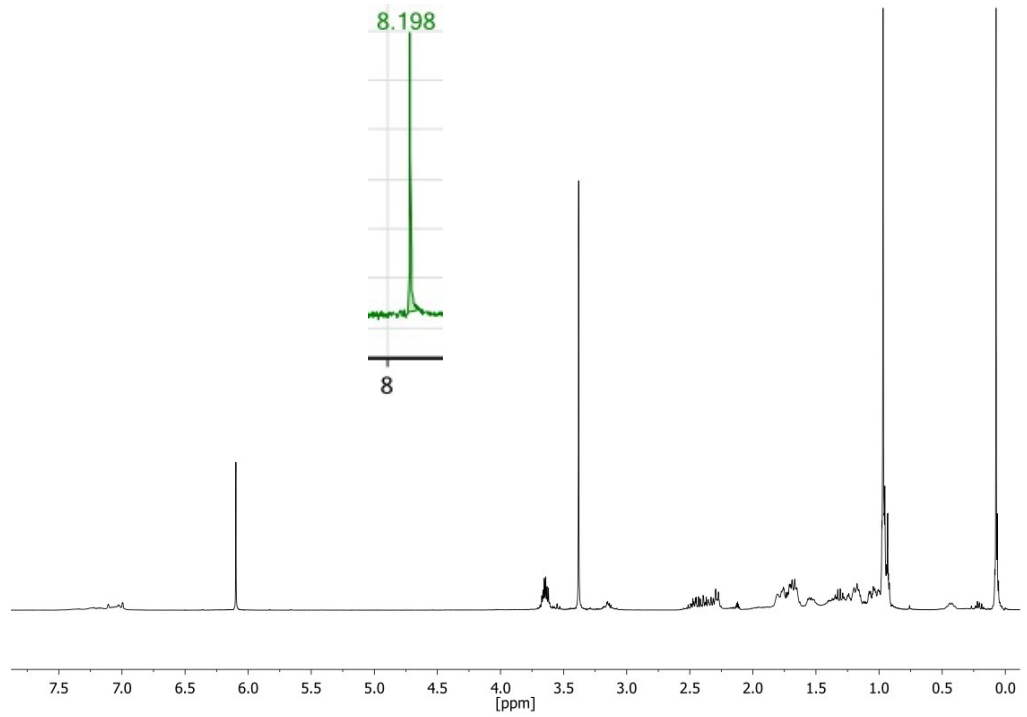

Figure S15. ^{1}H NMR spectrum (300 MHz, toluene-d_8, rt) and branched/linear selectivity via GC of **Entry 12**.

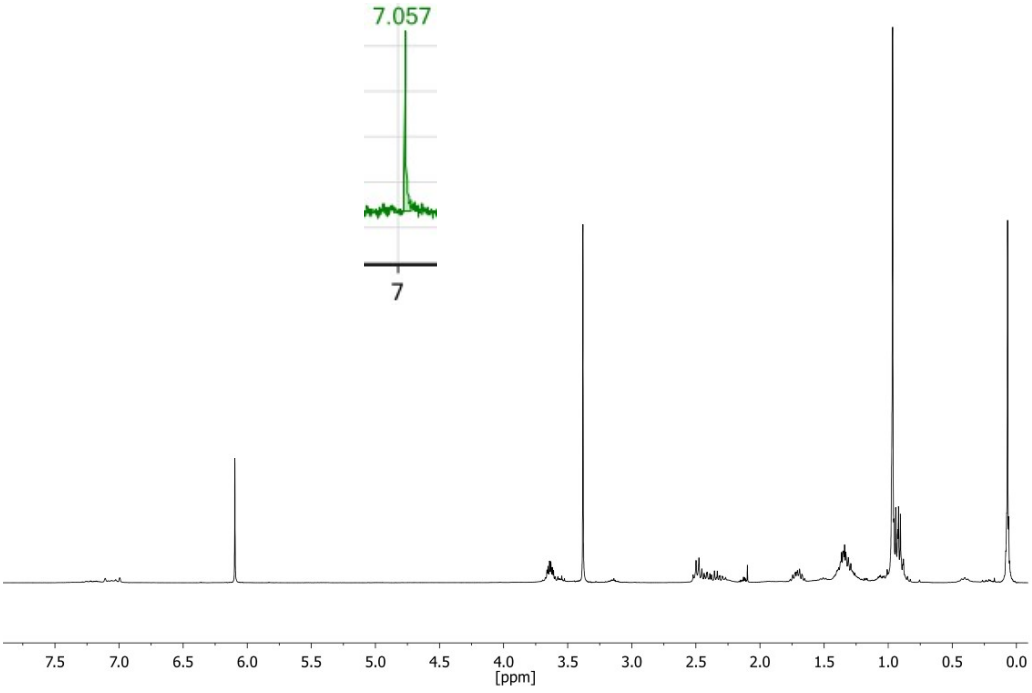

Figure S16. ^{1}H NMR spectrum (300 MHz, toluene-d_8, rt) and branched/linear selectivity via GC of **Entry 13**.

S3.2 Application in Fine Chemical Synthesis

2-(4-((tert-butyldimethylsilyl)oxy)butan-2-yl)-1,2,3,4-tetrahydroquinoline (11a)

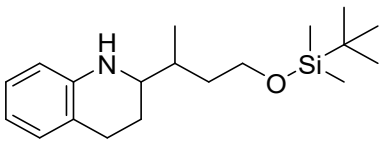

L1 (254 mg, 0.75 mmol) was weighed into a vial, dissolved in (but-3-en-1-yloxy)(*t*butyl)dimethylsilane (3.2 g, 18.8 mmol) and $Ti(NMe_2)_4$ (168 mg, 0.75 mmol) was added with a micropipette. After that, tetrahydroquinoline (1.0 g, 7.5 mmol) and was weighed into the same vial. The resultant reaction mixture was transferred into a high-pressure vial. The vial was placed into a preheated aluminium block at 160 °C for 24 h. The crude product (mixture of branched diastereomers and linear product (10:1)) was filtered through Celite and the residual alkene was removed *in vacuo* (can be reused). No further purification steps were needed for further use. The product **11a** was isolated as yellow oil (1.97 g, 6.2 mmol, 82%).

^{1}H NMR ($CDCl_3$, 400 MHz, rt): δ = 0.08 (s, 6 H, Si-(CH_3)$_2$), 0.92 (s, 9 H, C-(CH_3)$_3$), 0.99 (d, *J* = 6.6 Hz, 3 H, CH-CH_3), 1.28-2.00 (m, 5 H), 2.72-2.87 (m, 2 H), 3.17-3.27 (m, 1 H), 3.60-3.78 (m, 3 H), 6.47-6.49 (m, 1 H, Ar-*H*), 6.57-6.63 (m, 1 H, Ar-*H*), 6.95-6.99 (m, 2 H, Ar-*H*) ppm.

^{13}C NMR ($CDCl_3$, 101 MHz, rt): δ = -5.11 (Si-(CH_3)$_2$), 15.55 (CH-*C*H_3), 18.92 (*C*-(CH$_3$)$_3$), 24.55 (*C*H_2), 26.13 (C-(*C*H_3)$_3$), 27.16 (*C*H_2), 34.28 (*C*H-CH$_3$), 35.53 (*C*H_2), 56.26 (N-*C*H), 61.52 (O-*C*H_2), 114.09 (Ar-*C*H), 116.73 (Ar-*C*H), 121.52 (Ar-*C*), 126.83 (Ar-*C*H), 129.24 (Ar-*C*H), 145.28 (Ar-*C*) ppm.

HRMS (ESI): m/z calc. for $C_{19}H_{34}NOSi$ [M+H$^+$]: 320.2410. Found: 320.2405.

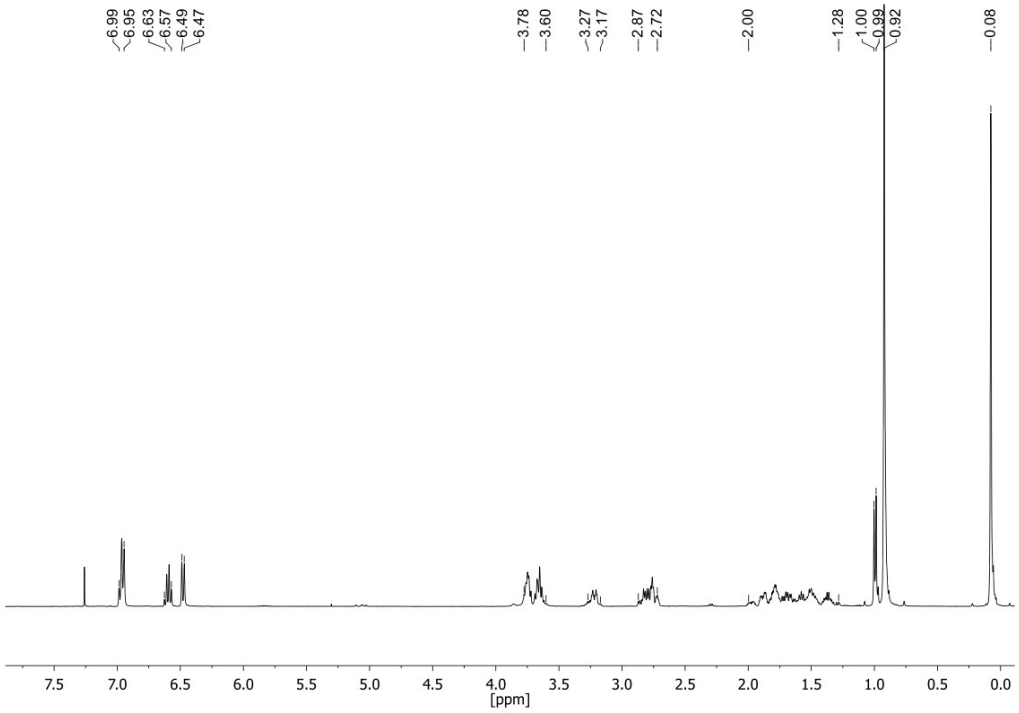

Figure S17. ^{1}H NMR spectrum (400 MHz, $CDCl_3$, rt) of **11a**.

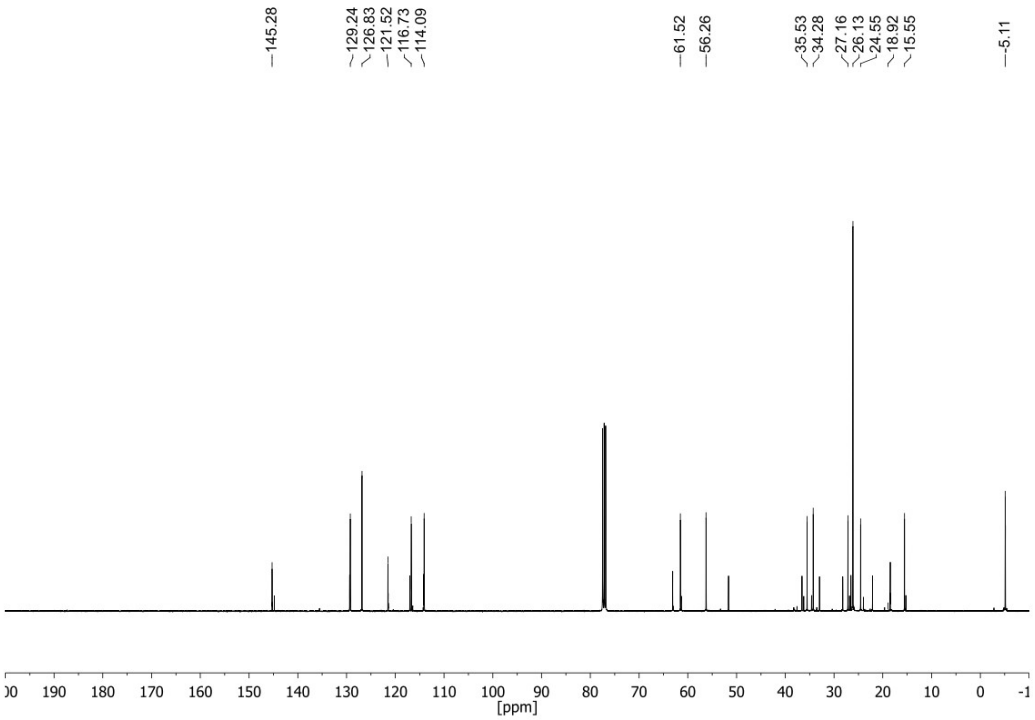

Figure S18. ^{13}C NMR spectrum (101 MHz, $CDCl_3$, rt) of **11a** (+signals of linear product).

3-methyl-1,2,3,3a,4,5-hexahydropyrrolo[1,2-a]quinoline (14a)

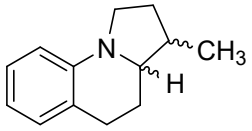

12a was prepared following a modified literature procedure.[2] **14a** (500 mg, 1.56 mmol) was dissolved in 20 mL acetonitrile,tosyl fluoride (815 mg, 4.68 mmol) and DBU (712 mg, 4.68 mmol) were added. The reaction mixture was heated to 90 °C for 48 h. The solution was cooled, diluted with 1M NaOH (30 mL), stirred at room temperature for 1 h and diluted with ethyl acetate (50 mL). The organic phase was then washed with water and brine, dried over $MgSO_4$ and concentrated *in vacuo*. The crude product was purified by chromatography (SiO_2, hexanes/DCM/cyclohexane = 1:2:2) and after removal of all volatiles *in vacuo*, the product **14a** was isolated as diastereomeric mixture (syn/anti = 1:4.8) as yellow oil (234 mg, 1.25 mmol, 80%).

^{1}H NMR ($CDCl_3$, 400 MHz, rt): δ = 1.01 (d, J = 7.1 Hz, 3 H, CH-CH_3), 1.62-1.73 (m, 1 H), 1.79-1.85 (m, 1 H), 1.98-2.03 (m, 1 H), 2.16-2.30 (m, 1 H), 2.41-2.49 (m, 1 H), 2.87-3.11 (m, 2 H), 3.27-3.48 (m, 2H), 3.64-3.69 (m, 1 H), 6.48-6.51 (m, 1 H, Ar-*H*), 6.64-6.68 (m, 1 H, Ar-*H*), 7.09-7.11 (m, 1 H, Ar-*H*), 7.17-7.21 (m, 1 H, Ar-*H*) ppm.

^{13}C NMR ($CDCl_3$, 101 MHz, rt): δ = 14.60 (CH-*C*H_3), 23.27 (*C*H_2), 28.47 (*C*H_2), 31.94 (*C*H_2), 35.76 (*C*H-CH_3), 45.12 (*C*H_2), 60.87 (N-*C*H), 109.85 (Ar-*C*H), 114.76 (Ar-*C*H), 121.37 (Ar-*C*), 127.37 (Ar-*C*H), 128.54 (Ar-*C*H), 145.39 (Ar-*C*) ppm.

HRMS (ESI): m/z calc. for $C_{13}H_{18}N$ [M+H$^+$]: 188.1439. Found: 188.1437.

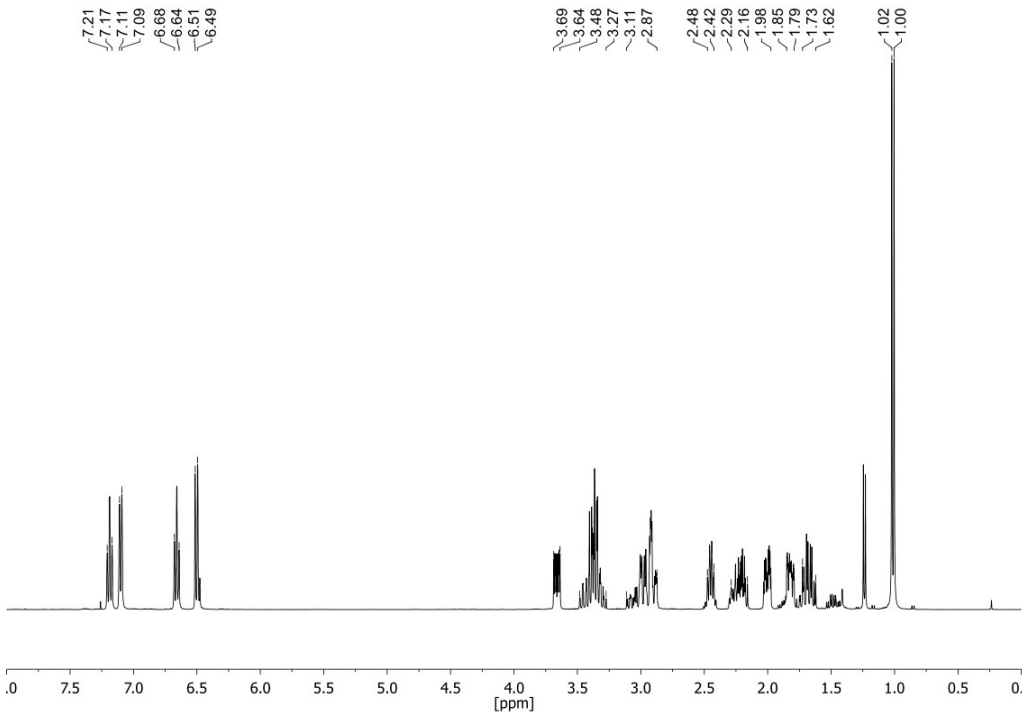

Figure S19. ^{1}H NMR spectrum (400 MHz, $CDCl_3$, rt) of **14a**.

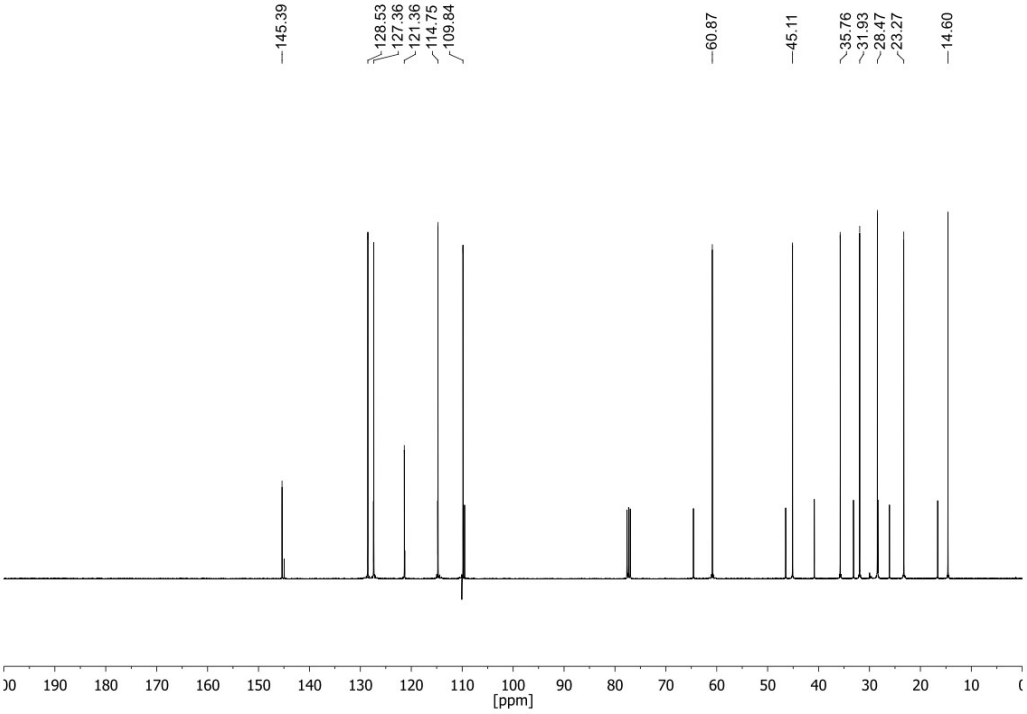

Figure S20. ^{13}C NMR spectrum (101 MHz, $CDCl_3$, rt) of **14a**.

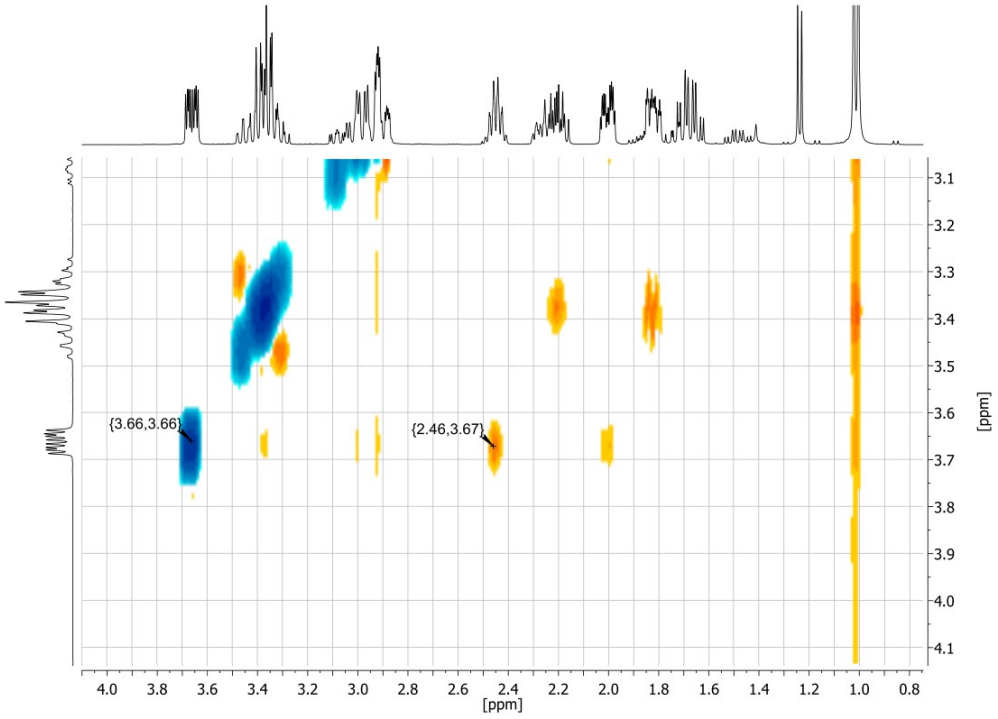

Figure S21. Selected signals from the NOESY spectrum ($CDCl_3$, rt) of **14a**.

2,3,4,4a,5,6-hexahydro-1H-pyrido[1,2-a]quinoline (14b)

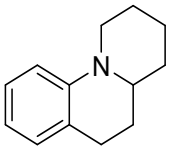

For preparation see **12a**. Product **14b** was isolated as yellow oil (15 mg, 0.08 mmol, 5%).

^{1}H NMR ($CDCl_3$, 400 MHz, rt): δ = 1.42-1.47 (m, 2 H), 1.58-1.85 (m, 5 H), 1.93-1.99 (m, 1 H), 2.65-2.74 (m, 2 H), 2.80-2.94 (m, 2 H), 3.94-3.97 (m, 1 H), 6.65-6.69 (m, 1 H, Ar-*H*), 6.83-6.85 (m, 1 H, Ar-*H*), 6.97-6.99 (m, 1 H, Ar-*H*), 7.08-7.12 (m, 1 H, Ar-*H*) ppm.

^{13}C NMR ($CDCl_3$, 101 MHz, rt): δ = 24.63 (CH_2), 25.91 (CH_2), 27.19 (CH_2), 30.39 (CH_2), 33.48 (CH_2), 48.27 (N-CH_2), 57.03 (N-CH), 112.90 (Ar-CH), 117.34 (Ar-CH), 125.00 (Ar-*C*), 127.00 (Ar-CH), 129.13 (Ar-CH), 146.98 (Ar-*C*) ppm.

HRMS (ESI): m/z calc. for $C_{13}H_{18}N$ [M+H$^+$]: 188.1439. Found: 188.1434.

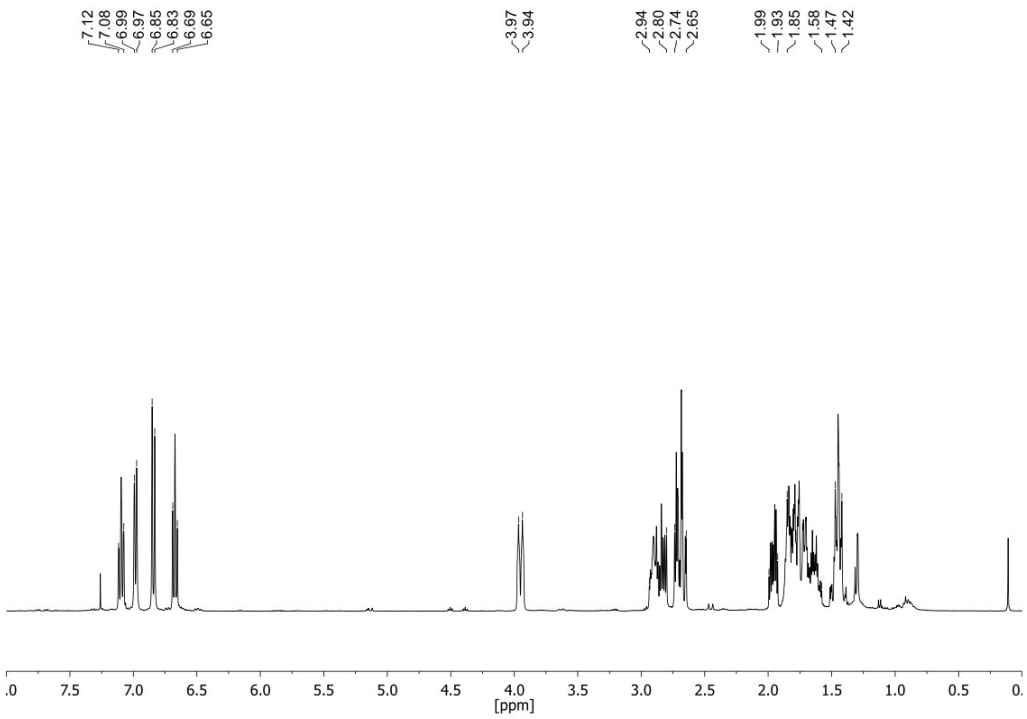

Figure S22. ^{1}H NMR spectrum (400 MHz, $CDCl_3$, rt) of **14b**.

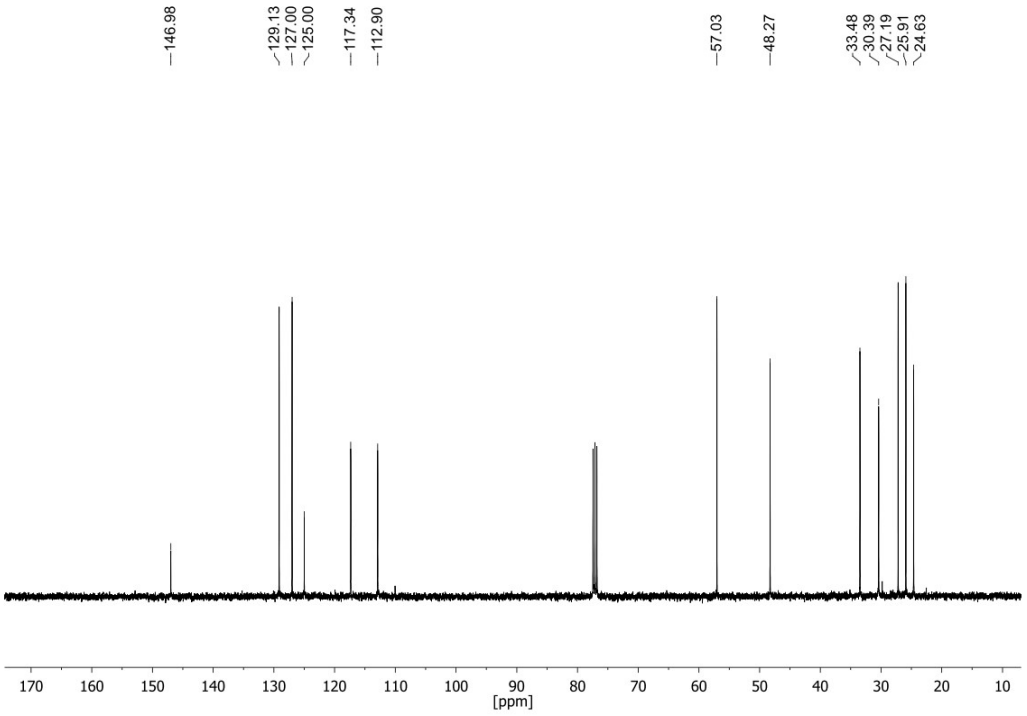

Figure S23. ^{13}C NMR spectrum (101 MHz, $CDCl_3$, rt) of **14b**.

S3.3 Application in Post-Polymerization Amination of Vinyl Terminated Polypropylene

General Procedure of AT230/AT350-HNMePh/HNMeBu/HNMeCy Syntheses (0.10-1.0 g): **L1** and $Ti(NMe_2)_4$ were weighed into separate 1-dram vials, and $Ti(NMe_2)_4$ was quantitatively transferred into the vial containing **L1** with 300 µL of pre-dried toluene to generate a red solution. The amine substrate was weighed into a separate 1-dram vial and quantitatively transferred into the vial containing the catalyst solution with 200 µL of pre-dried toluene. A thick-walled vessel containing either **VT230** or **VT350** was charged with the catalyst-amine solution. The reaction was heated to 160 °C with a silicon oil baith and agitated with a Teflon coated stir bar over a magnetic stir plate for three days. The reaction was cooled to room temperature and collected with hexanes and stirred over MeOH to quench the catalyst. Solvents were removed under reduced pressure and the product was filtered through a 1-inch silica pad with hexanes. Any residual ligand could be further removed by removing solvents again under reduced pressure and filtering through a short Celite plug with minimal amounts of hexanes. The crude product of **AT350-HNMeBu** could not be purified by these procedures and was purified by chromatography (SiO_2, hexanes/EtOAc = 1:1) and after removal of all volatiles *in vacuo*, the product was isolated as a yellow oil. Purified products were then dried *in vacuo* at 30 °C overnight prior to characterization.

General Procedure of AT840/AT7200-HNMePh/HNMeBu/HNMeCy Syntheses (1.0-5.0 g): **L1** and $Ti(NMe_2)_4$ were weighed into separate 1-dram vials, and $Ti(NMe_2)_4$ was quantitatively transferred into the vial containing **L1** with 300 µL of pre-dried toluene to generate a red solution. The amine substrate was weighed into a separate 1-dram vial and quantitatively transferred into the vial containing the catalyst solution with 200 µL of pre-dried toluene. A thick-walled vessel containing either **VT230** or **VT350** was charged with the catalyst-amine solution. The reaction was heated to 160 °C with a silicon oil baith and agitated with a Teflon coated stir bar over a magnetic stir plate for five days. The reaction was cooled to room temperature and collected with hexanes and stirred over MeOH to quench the catalyst. Solvents were removed under reduced pressure and the product was filtered through a 1-inch silica plug with hexanes. The products were then precipitated from concentrated DCM solutions in cold MeOH three times to remove residual proteo-ligand. Purified products were then dried *in vacuo* at 50 °C overnight prior to characterization.

Table S3. Reaction scope and conditions of $Ti(NMe_2)_4$/**L1** catalyzed hydroaminoalkylation of VTPPs.

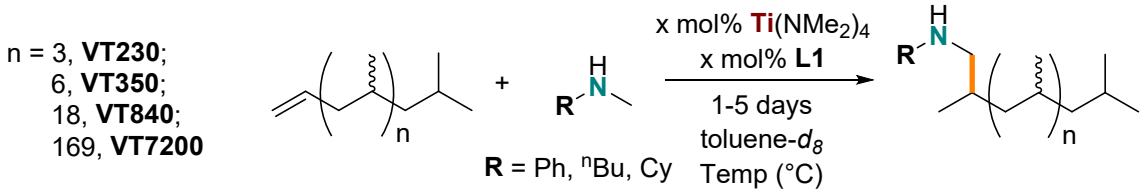

Entry	VT	n (number average)	Mass (g)	R	x	Temp (°C)	Yield (g,%)
1	230	3	0.10	Ph	5	160	0.12, 82%
2	230	3	0.10	^{n}Bu	10	160	0.10, 73%
3	230	3	0.10	Cy	10	160	0.11, 74%

4	350	5	1.00	Ph	10	160	0.88, 68%
5	350	5	1.00	^{n}Bu	15	160	0.41, 32%
6	350	5	1.00	Cy	10	160	1.04, 77%
7	840	22	5.00	Ph	10	160	4.70, 83%
8	840	22	5.00	^{n}Bu	15	160	3.77, 68%
9	840	22	5.00	Cy	20	160	1.68, 30%
10	7200	169	1.20	Ph	20	160	0.92, 76%
11	7200	169	1.50	^{n}Bu	30	180	1.15, 76%
12	7200	169	1.25	Cy	25	160	0.74, 59%

AT230-HNMePh/HNMeBu/HNMeCy as an Example of ^{1}H and ^{13}C NMR Analysis of Amine Terminated Polypropylene.

Assignment of ^{1}H and ^{13}C{^{1}H} NMR spectroscopy resonances are based on previously reported characterization of ATPP materials.[3]

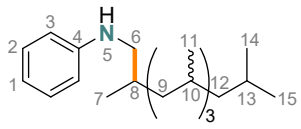

^{1}H NMR (300 MHz, $CDCl_3$, 298 K) δ = 0.90 (m, br, 19H, **H11**); 1.01 (m, br, 15H, **H9**); 1.66 (m, br, 5H, **H10**); 1.89 (m, br, 1H, **H8**); 3.09-2.91 (d of m, 2H, **H6**); 3.69 (s, br, 1H, **H5**); 6.65 (d, 1H, **H1**); 6.72 (t, 2H, **H3**); 7.21 (t, 2H, **H2**) ppm. Undetermined: **H7**, **H12**, **H13**, **H14**, **H15**. **^{13}C{^{1}H} NMR** (300 MHz, $CDCl_3$, 298 K) δ = 23.8-21.3 (multiple s, **C11**); 25.3 (s, **C13**); 27.7-27.3 (multiple s, **C10**); 30.5 (s, **C8**); 48.0-42.6 (multiple s, **C9**); 51.2-50.6 (s, **C6**); 112.8 (s, **C3**); 117.1 (s, **C1**); 129.3 (s, **C2**); 148.7 (s, **C4**) ppm. Undetermined: **C7**, **C12**, **C14**, **C15**.

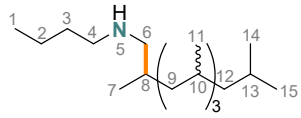

^{1}H NMR (300 MHz, $CDCl_3$, 298 K) δ = 0.88-0.79 (m, br, 35H, **H11** overlapping with **H1**); 0.91 (t, **H1** overlapping with **H11**); 1.26-0.90 (m, br, 13H, **H9**); 1.32 (m, 2H, **H2**); 1.56 (m, br, 9H, **H10** & **H3** overlapping); 1.75 (m, br, 1H, **H8**); 2.60-2.36 (d of m, 2H, **H6**); 2.60 (t, 2H, **H4**) ppm. Undetermined: **H5**, **H7**, **H12**, **H13**, **H14**, **H15**. **^{13}C{^{1}H} NMR** (300 MHz, $CDCl_3$, 298 K) δ = 14.2 (s, **C1**); 20.7 (s, **C2**); 24.0-17.9 (multiple s, **C11**); 25.3 (s, **C13**); 27.7-27.4 (multiple s, **C10**); 30.7 (s, **C8**); 32.4 (s, **C3**); 48.1-42.3 (multiple s, **C9**); 50.1-50.0 (s, **C4**); 57.7-56.6 (s, **C6**) ppm. Undetermined: **C7**, **C12**, **C14**, **C15**

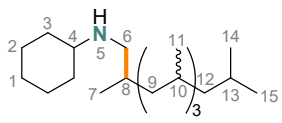

^{1}H NMR (300 MHz, $CDCl_3$, 298 K) δ = 0.81 (m, br, 24H, **H11**); 1.26-1.01 (m, br, 14H, **H1**, **H2**, **H9**, **H3** overlapping);1.72-1.50 (m, br, 9H, **H1**, **H2**, **H8**, **H10**, **H13**); 1.86-1.82 (d, br, 2H **H3**); 2.57 (t, 2H, **H4**); 2.62-2.28 (d of m, 2H, **H6**) ppm. Undetermined: **H5**, **H7**, **H12**, **H14**, **H15**. **^{13}C{^{1}H} NMR** (300 MHz, $CDCl_3$, 298 K) δ = 23.9-18.0 (multiple s, **C11**); 25.2 (2 s overlapping, **C2** & **C13**); 26.3 (s, **C1**); 27.6-27.3 (multiple s, **C10**); 30.9 (s, br, **C8**); 33.7 (s, br, **C3**); 48.0-42.8 (multiple s, **C9**); 54.6-53.5 (s, **C6**); 57.0 (s, **C4**) ppm. Undetermined: **C7**, **C12**, **C14**, **C15**

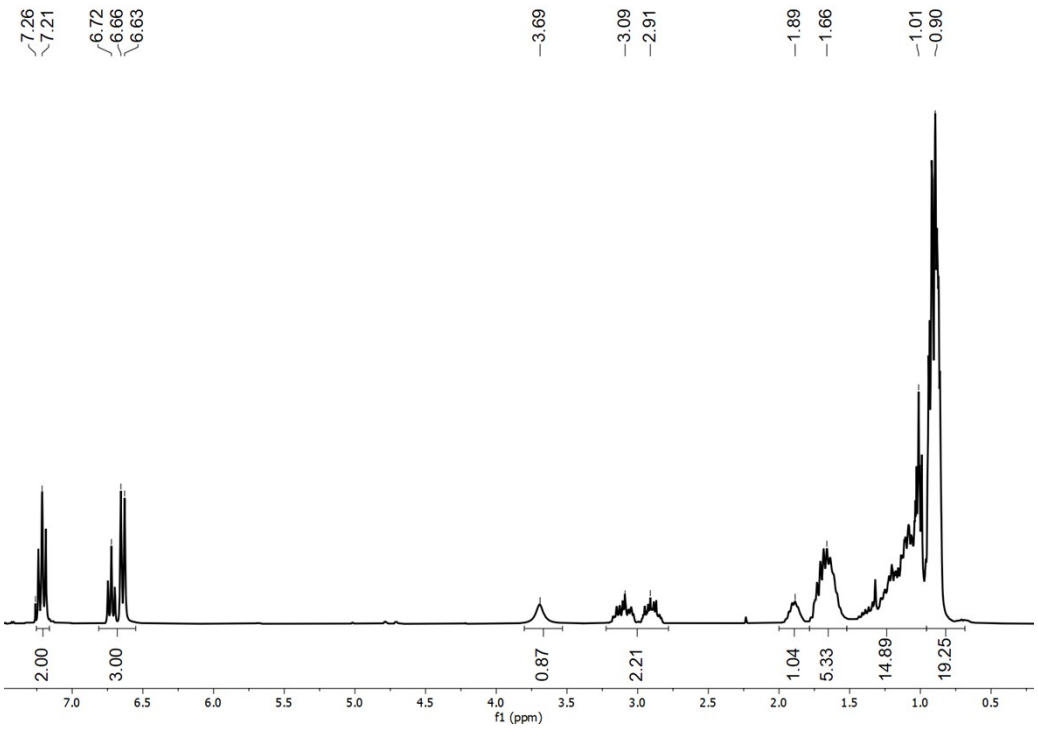

Figure S24. ^{1}H NMR spectrum (300 MHz, $CDCl_3$, 298 K) of **A230-HNMePh**.

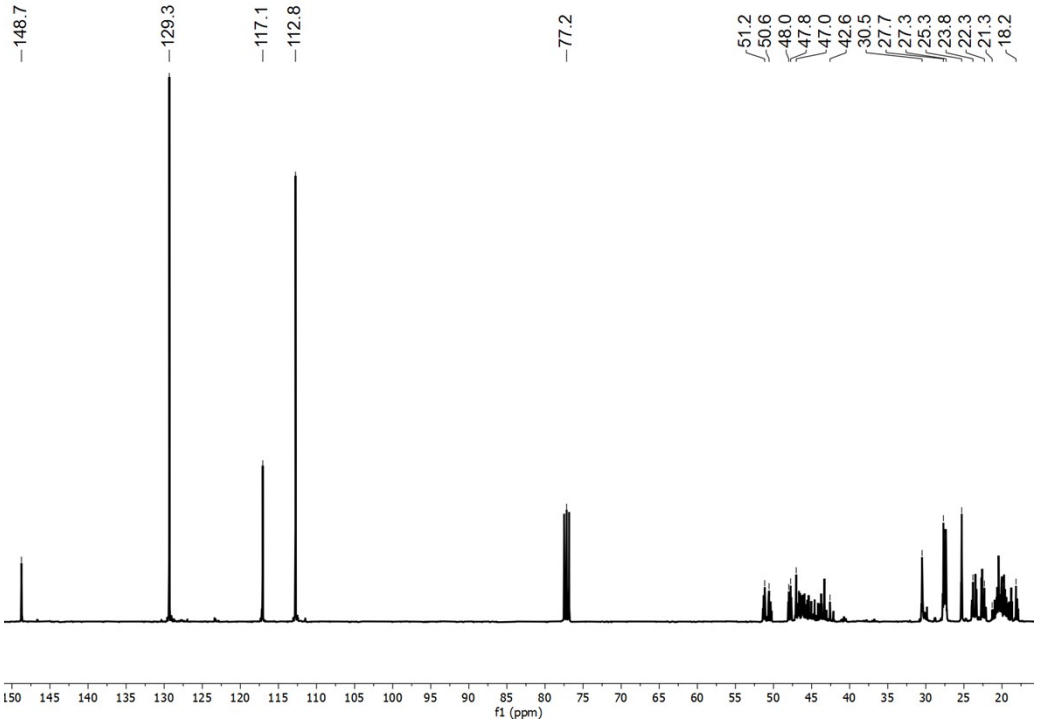

Figure S25. $^{13}C\{^{1}H\}$ NMR spectrum (101 MHz, $CDCl_3$, 298 K) of **A230-HNMePh**.

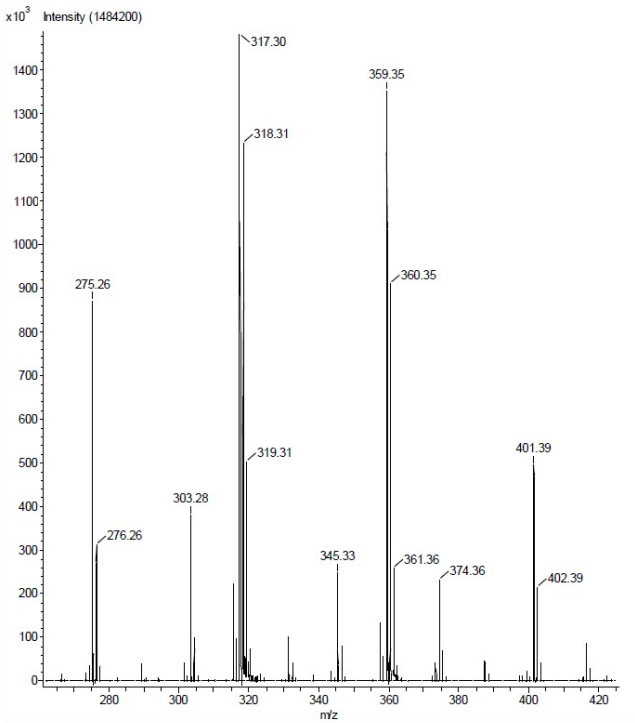

Figure S26. Low resolution field desorption mass spectrum of **AT230-HNMePh**. LRMS (FD) m/z: Calcd for $C_{22}H_{39}N$ 317.31; Found 317.30.

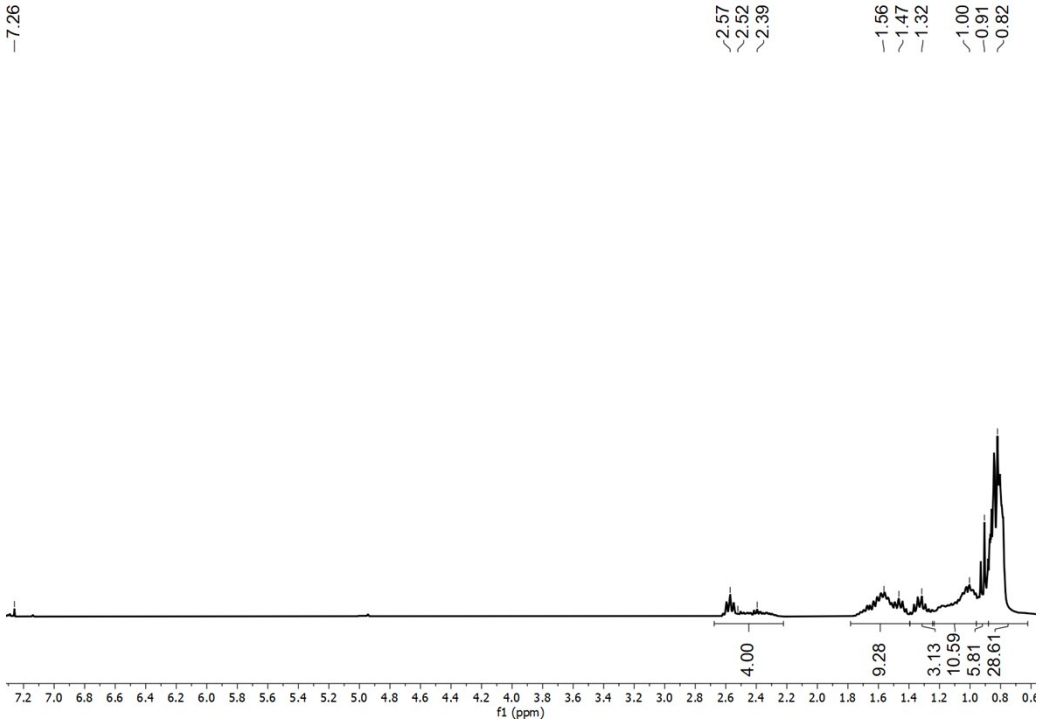

Figure S27. ^{1}H NMR spectrum (300 MHz, $CDCl_3$, 298 K) of **A230-HNMeBu**.

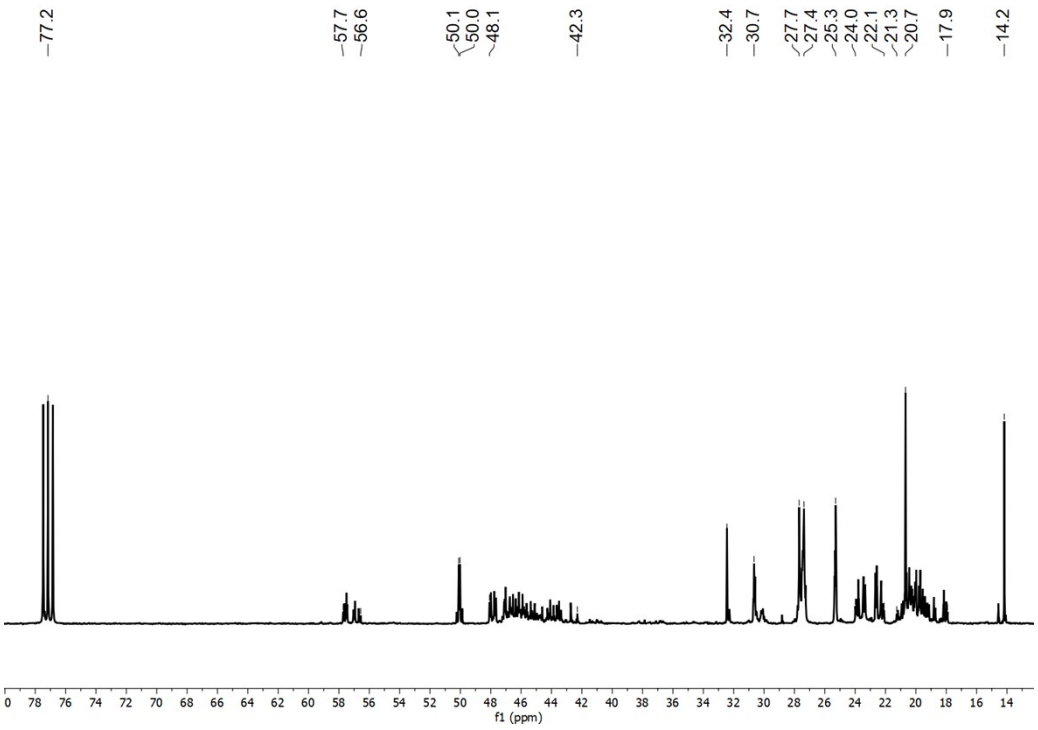

Figure S28. $^{13}C\{^{1}H\}$ NMR spectrum (101 MHz, $CDCl_3$, 298 K) of **A230-HNMeBu**.

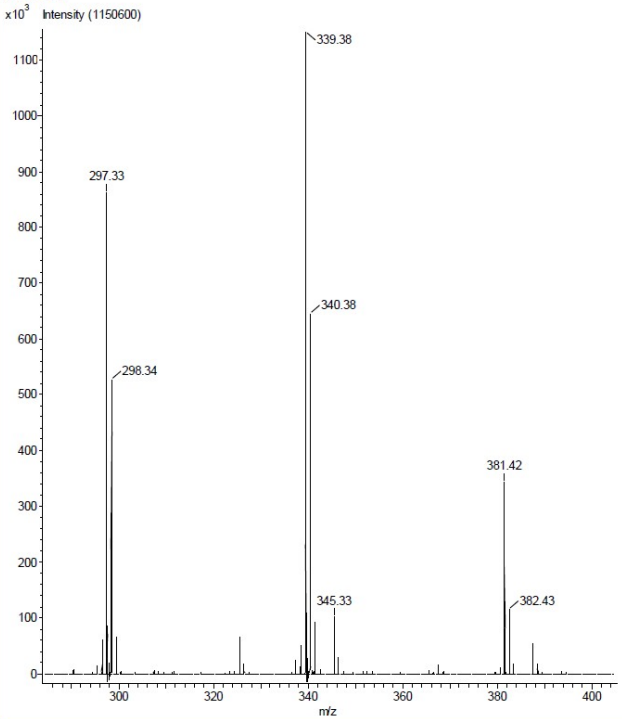

Figure S29. Low resolution field desorption mass spectrum of **AT230-HNMeBu**. LRMS (FD) m/z: Calcd for $C_{20}H_{43}N$ 297.34; Found 297.33.

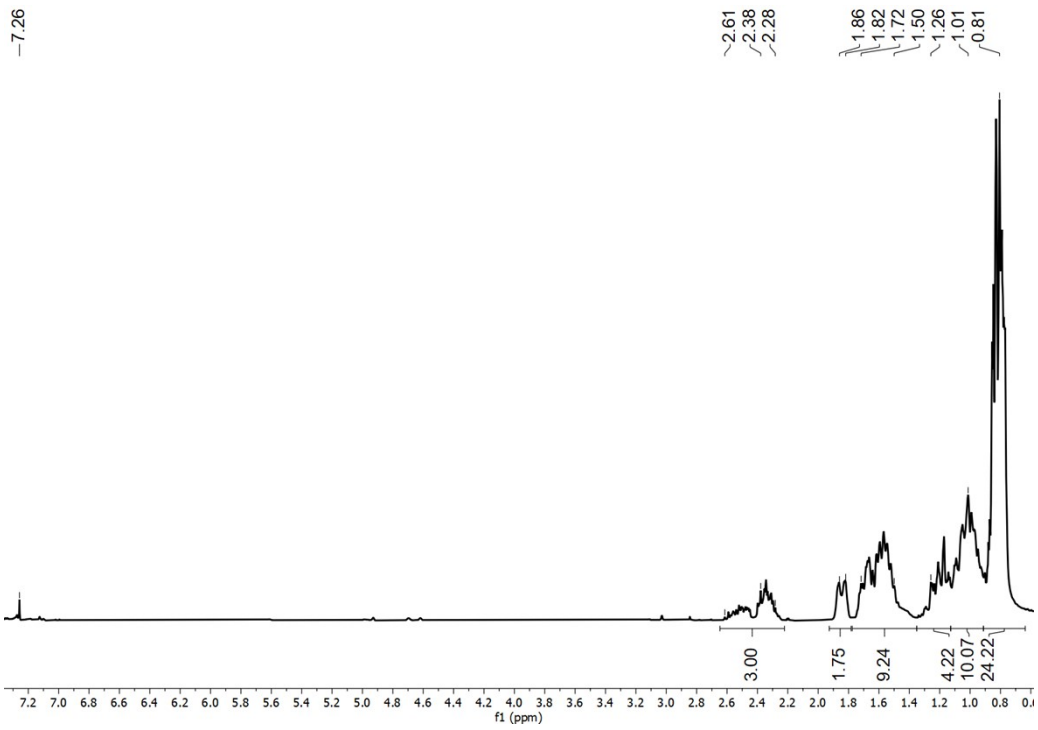

Figure S30. ^{1}H NMR spectrum (300 MHz, $CDCl_3$, 298 K) of **A230-HNMeCy**.

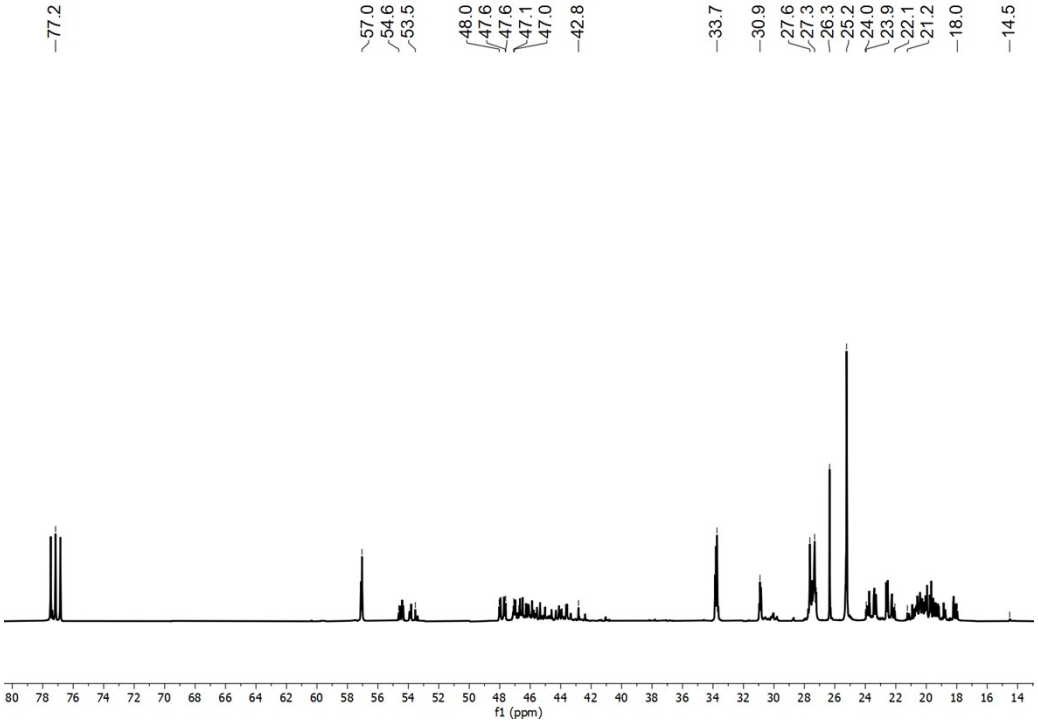

Figure S31. $^{13}C\{^{1}H\}$ NMR spectrum (101 MHz, $CDCl_3$, 298 K) of **A230-HNMeCy**.

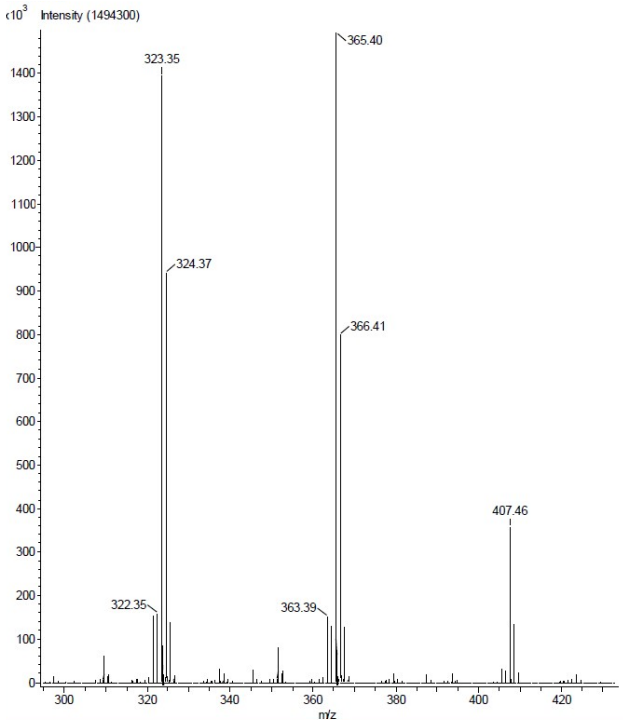

Figure S32. Low resolution field desorption mass spectrum of **AT230-HNMeCy**. LRMS (FD) m/z: Calcd for $C_{22}H_{45}N$ 323.36; Found 323.35.

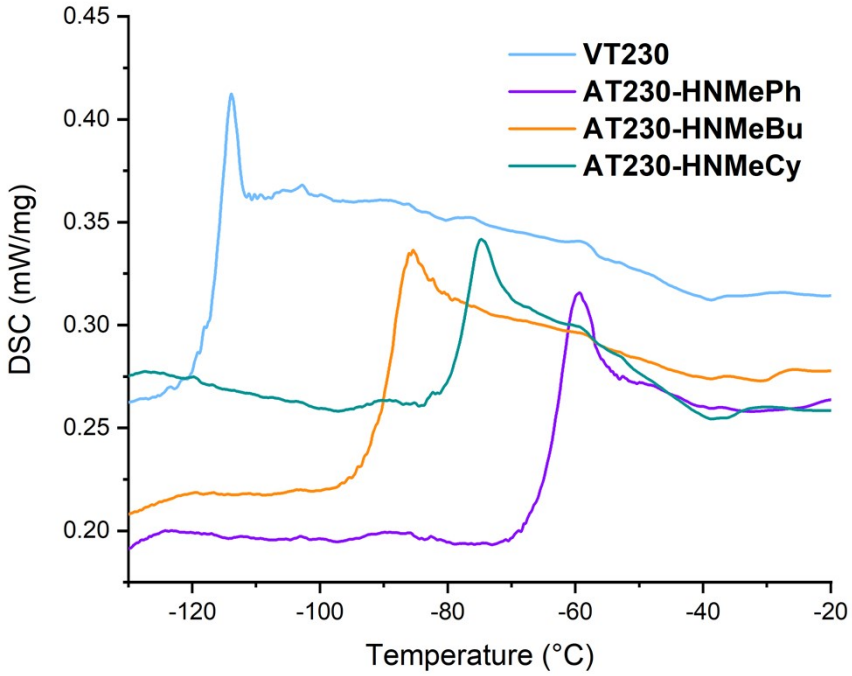

Figure S33. Overlaid DSC thermograms of **VT230** and **AVT230-HNMePh/HNMeBu/HNMeCy**.

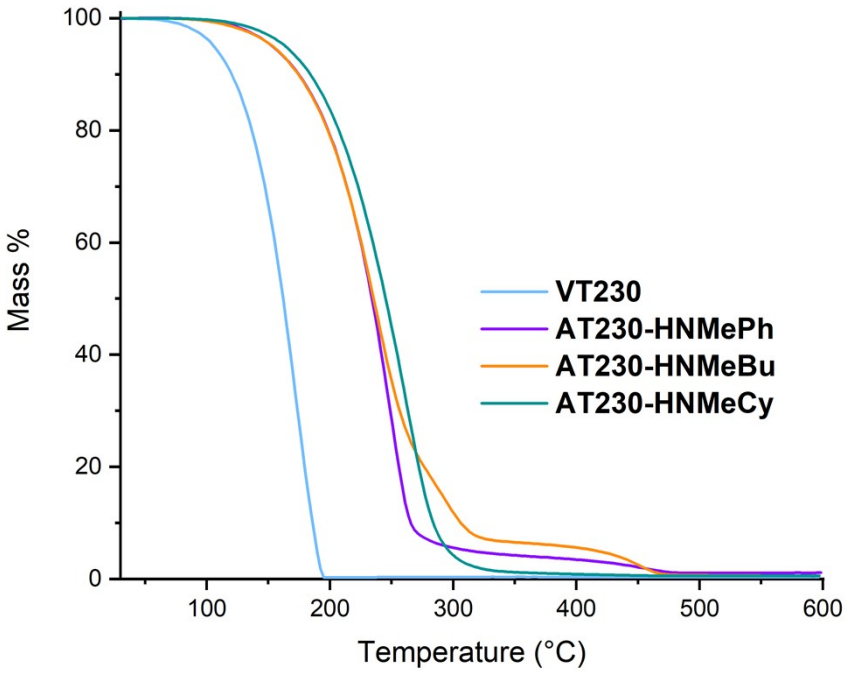

Figure S34. Overlaid TGA thermograms of **VT230** and **AVT230-HNMePh/HNMeBu/HNMeCy**.

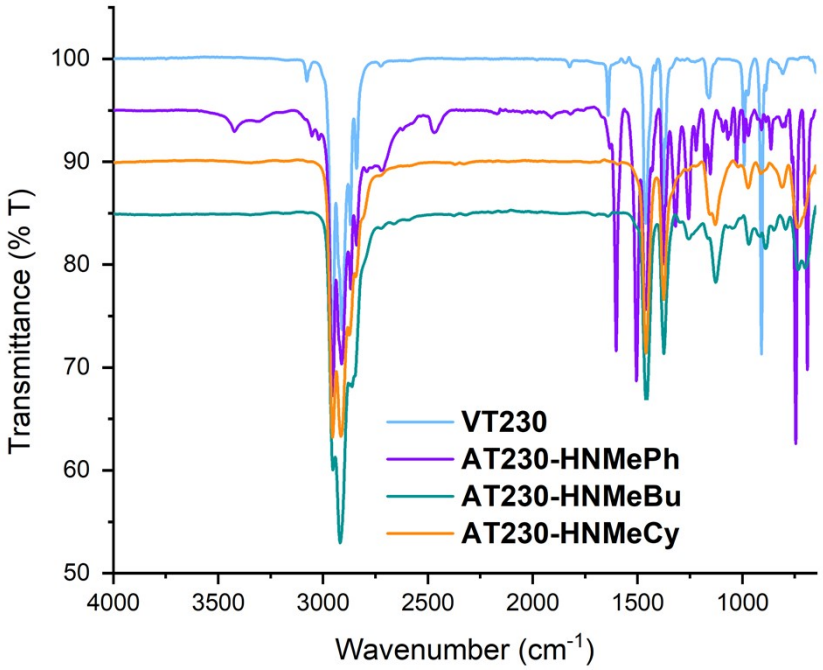

Figure S35. Overlaid IR spectra of **VT230** and aminated analogues **AT230-HNMePh/HNMeBu/HNMeCy**.

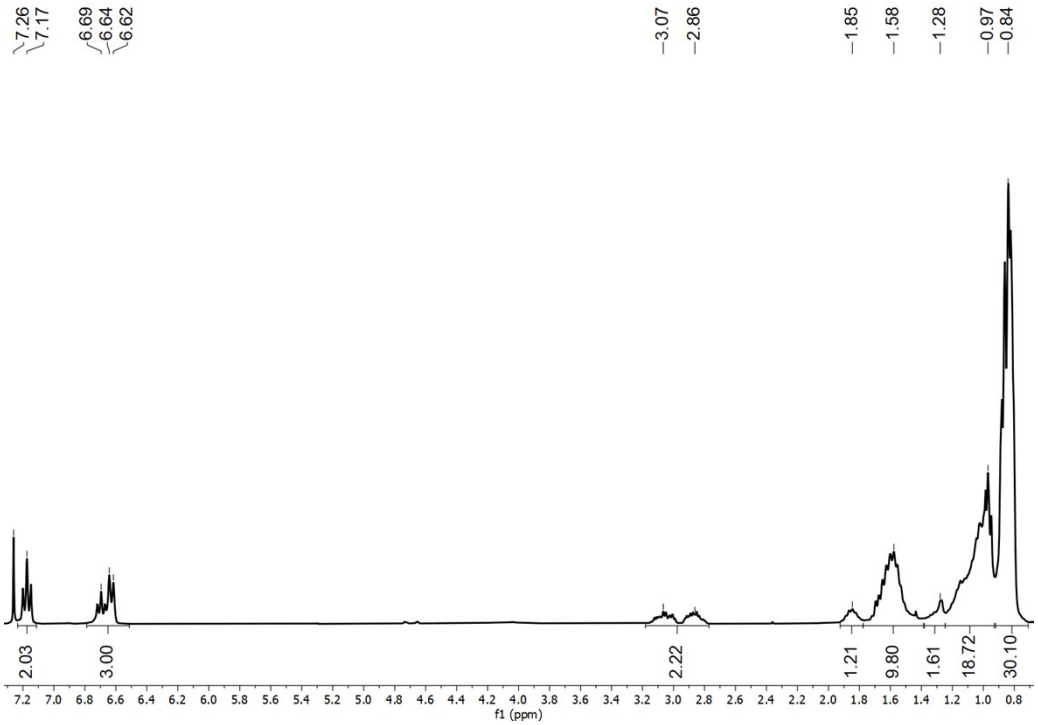

Figure S36. ^{1}H NMR spectrum (300 MHz, $CDCl_3$, 298 K) of **A350-HNMePh**.

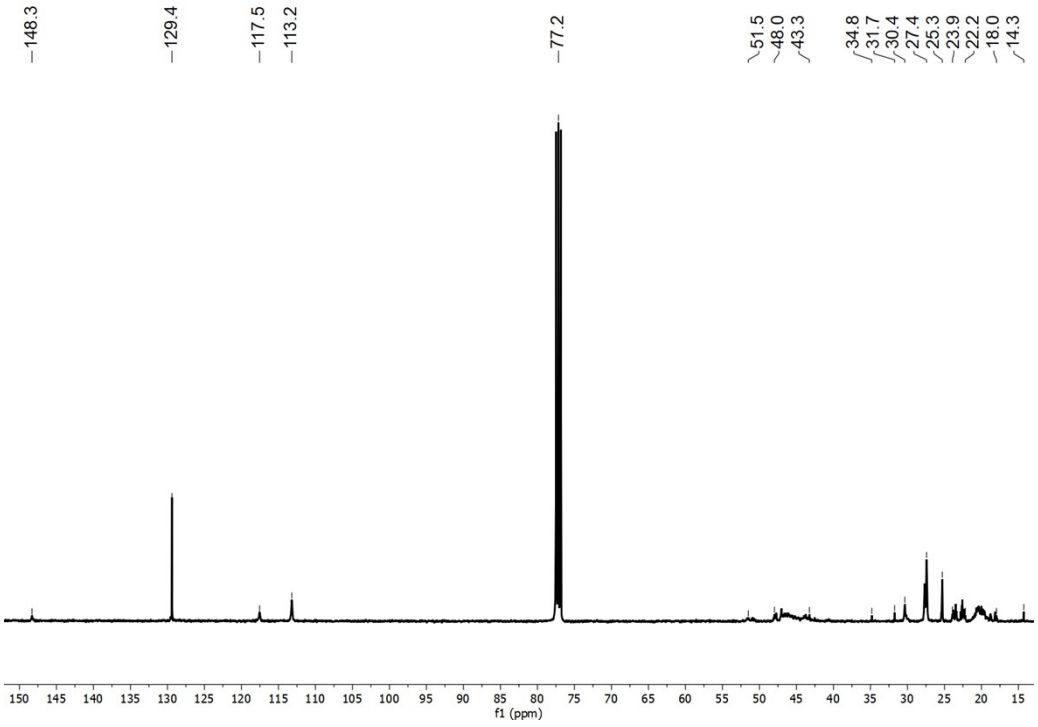

Figure S37. $^{13}C\{^{1}H\}$ NMR spectrum (101 MHz, $CDCl_3$, 298 K) of **A350-HNMePh**.

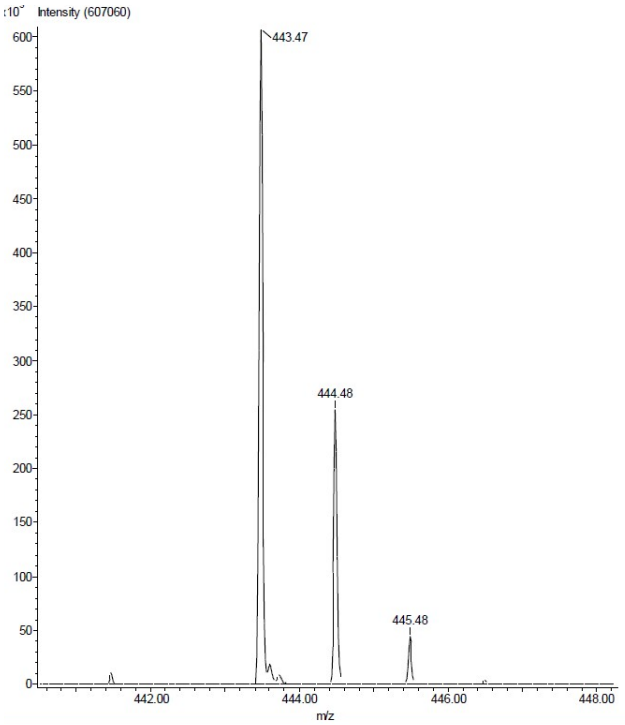

Figure S38. Low resolution field desorption mass spectrum of **AT350-HNMePh**. LRMS (FD) m/z: Calcd for $C_{31}H_{57}N$ 443.45; Found 443.47.

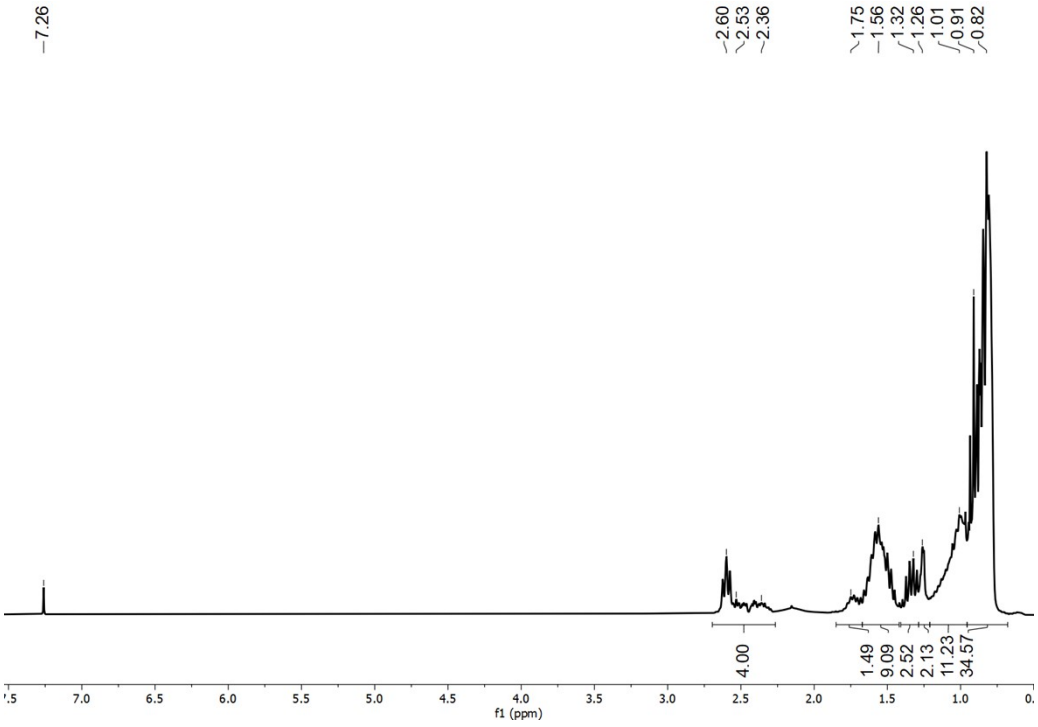

Figure S39. ^{1}H NMR spectrum (300 MHz, $CDCl_3$, 298 K) of **A350-HNMeBu**.

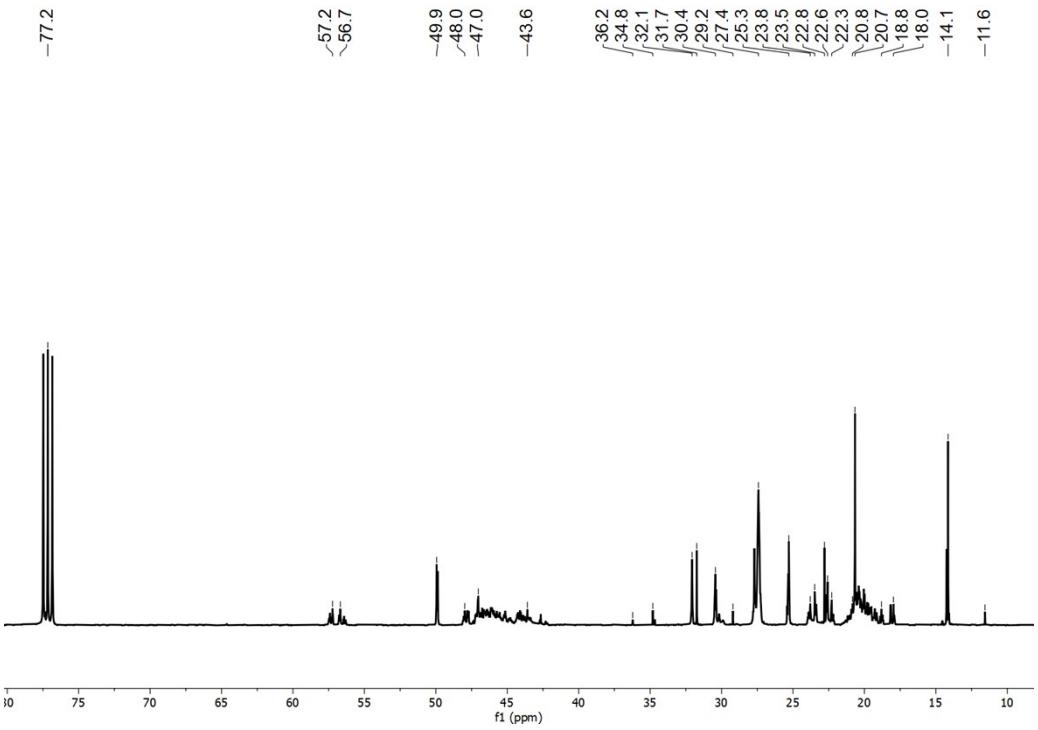

Figure S40. $^{13}C\{^{1}H\}$ NMR spectrum (101 MHz, $CDCl_3$, 298 K) of **A350-HNMeBu**.

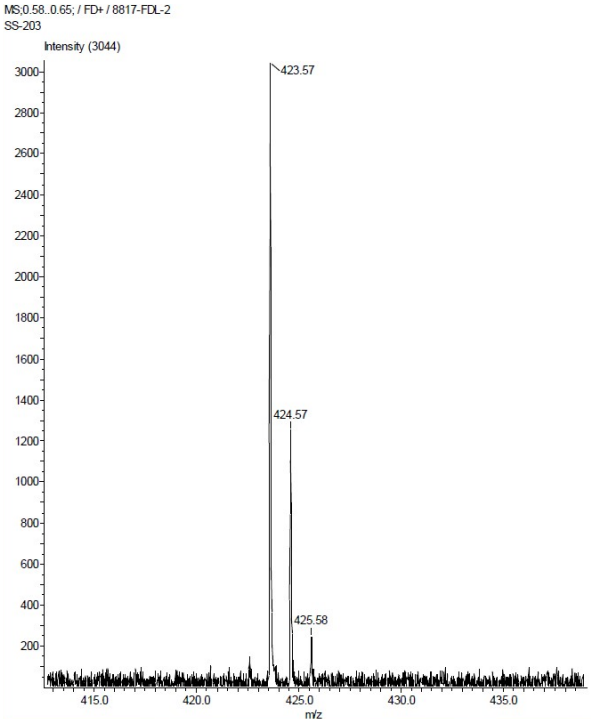

Figure S41. Low resolution field desorption mass spectrum of **AT350-HNMeBu**. LRMS (FD) m/z: Calcd for $C_{31}H_{63}N$ 423.48; Found 423.57.

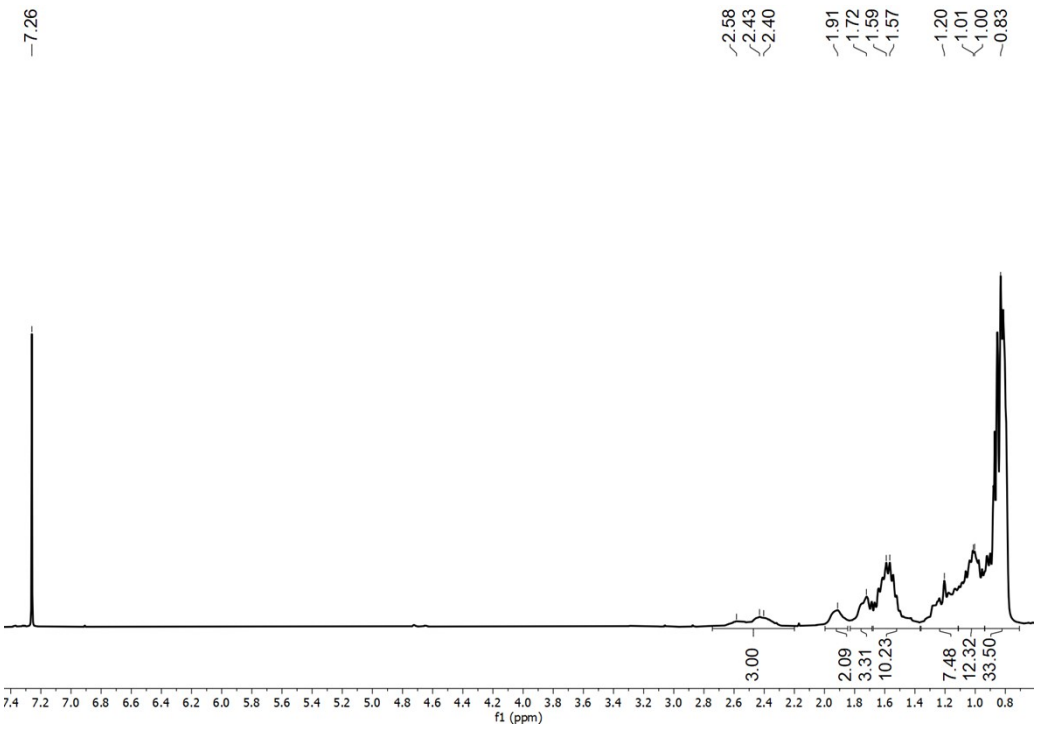

Figure S42. ^{1}H NMR spectrum (300 MHz, $CDCl_3$, 298 K) of **A350-HNMeCy**.

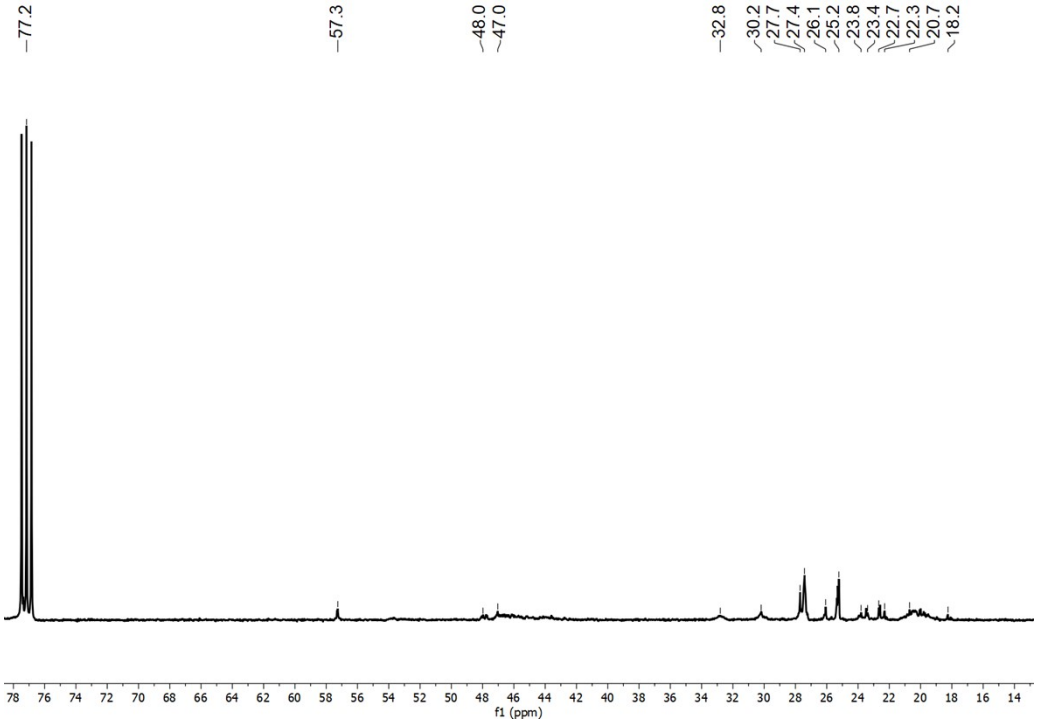

Figure S43. $^{13}C\{^{1}H\}$ NMR spectrum (101 MHz, $CDCl_3$, 298 K) of **A350-HNMeCy**.

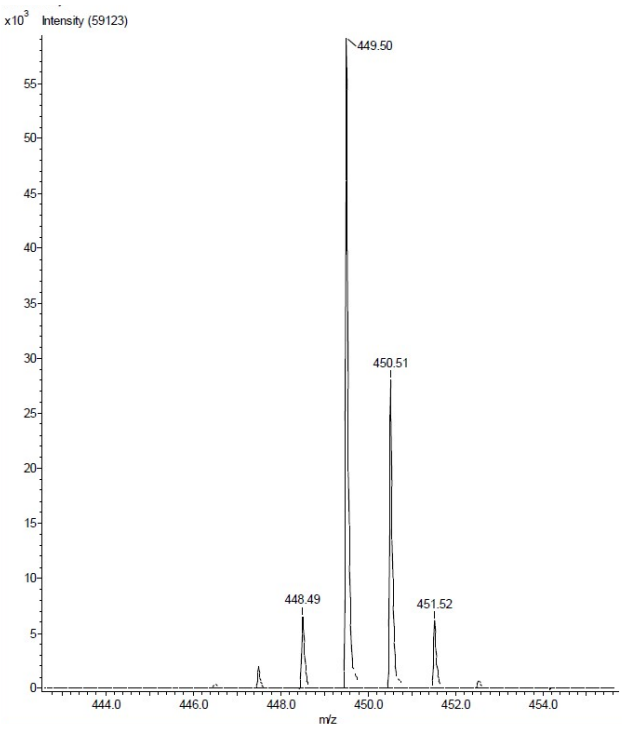

Figure S44. Low resolution field desorption mass spectrum of **AT350-HNMeCy**. LRMS (FD) m/z: Calcd for $C_{31}H_{63}N$ 449.50; Found 449.50.

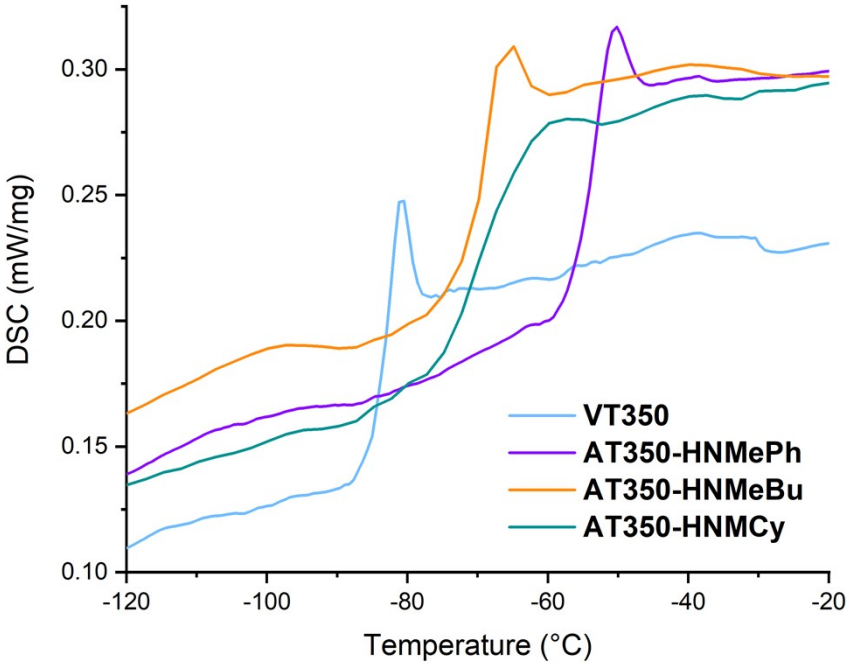

Figure S45. Overlaid DSC thermograms of **VT350** and **AVT350-HNMePh/HNMeBu/HNMeCy**.

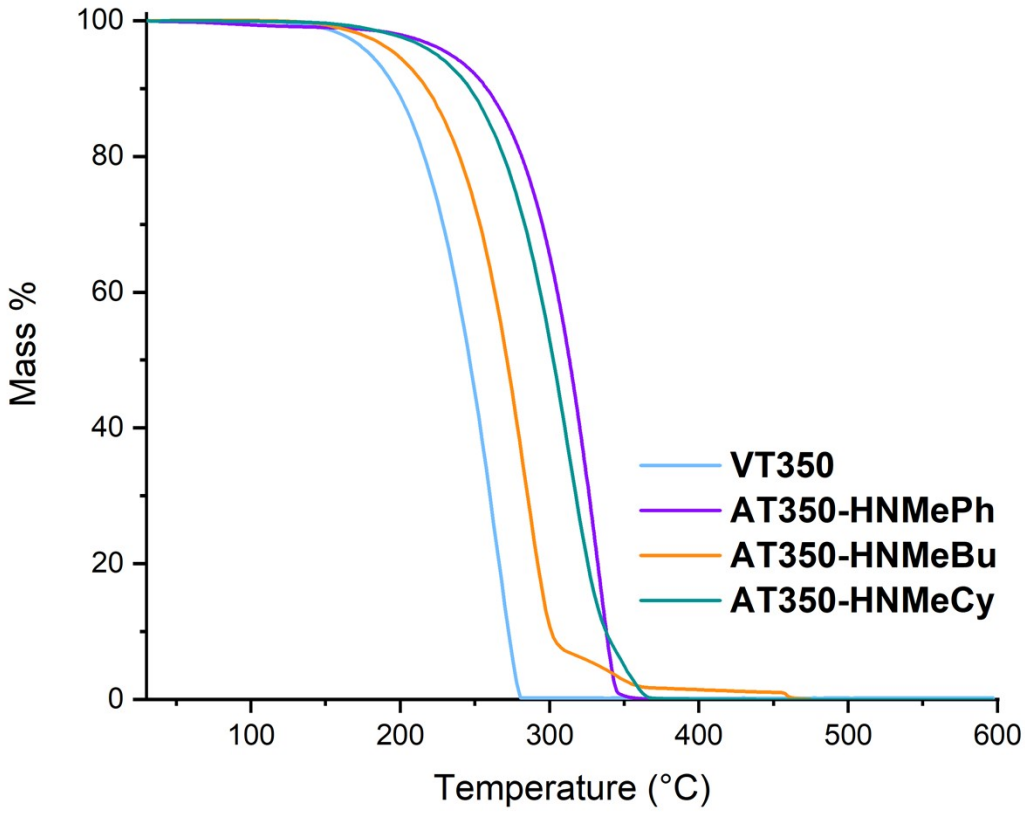

Figure S46. Overlaid TGA thermograms of **VT350** and **AVT350-HNMePh/HNMeBu/HNMeCy**.

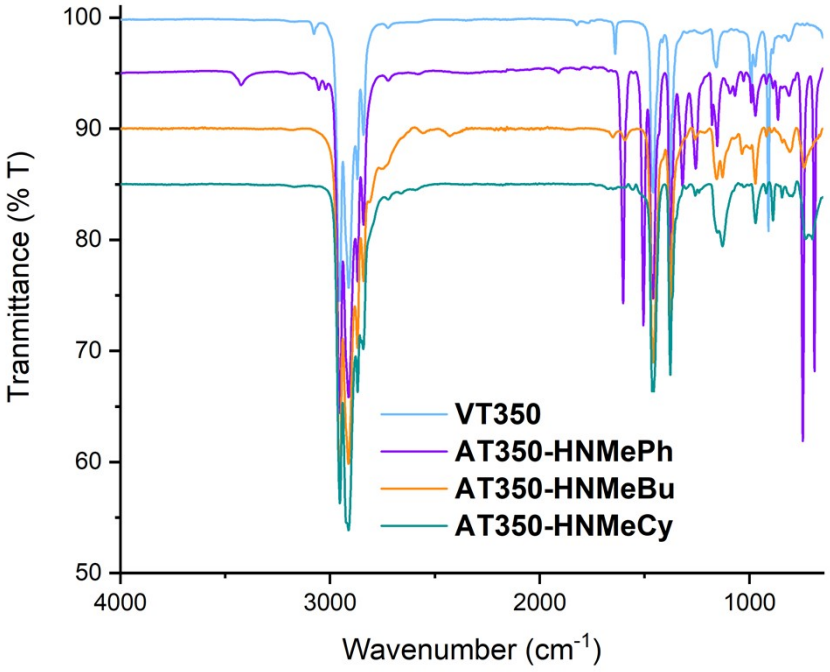

Figure S47. Overlaid IR spectra of **VT350** and aminated analogues **AT350-HNMePh/HNMeBu/HNMeCy**.

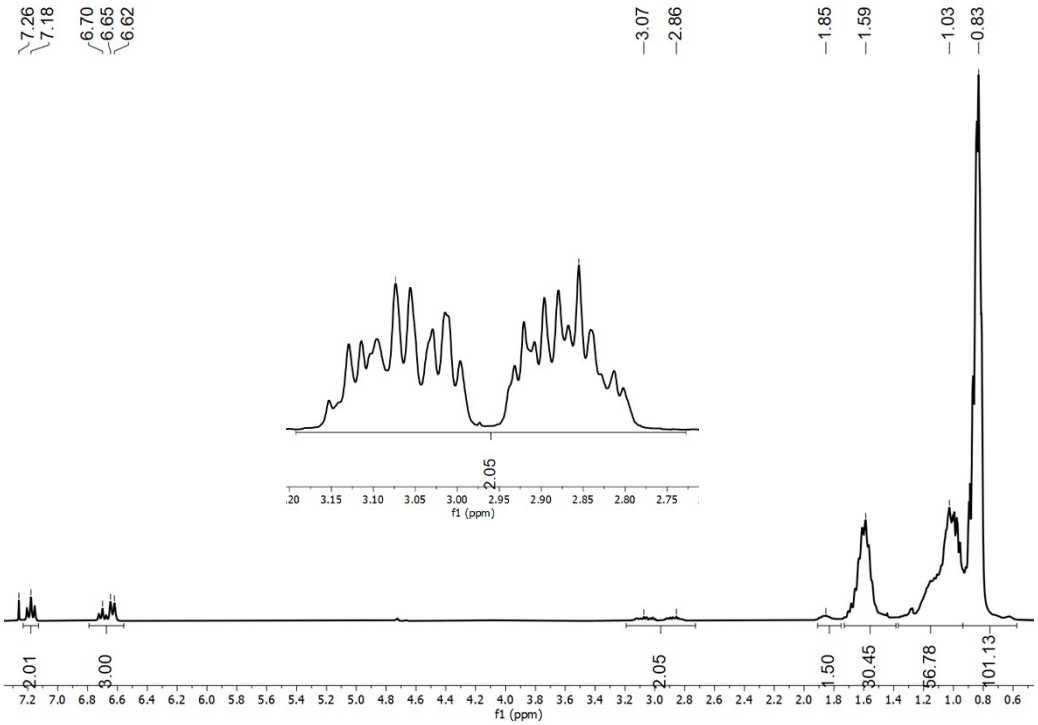

Figure S48. ^{1}H NMR spectrum (300 MHz, $CDCl_3$, 298 K) of **AT840-HNMePh**.

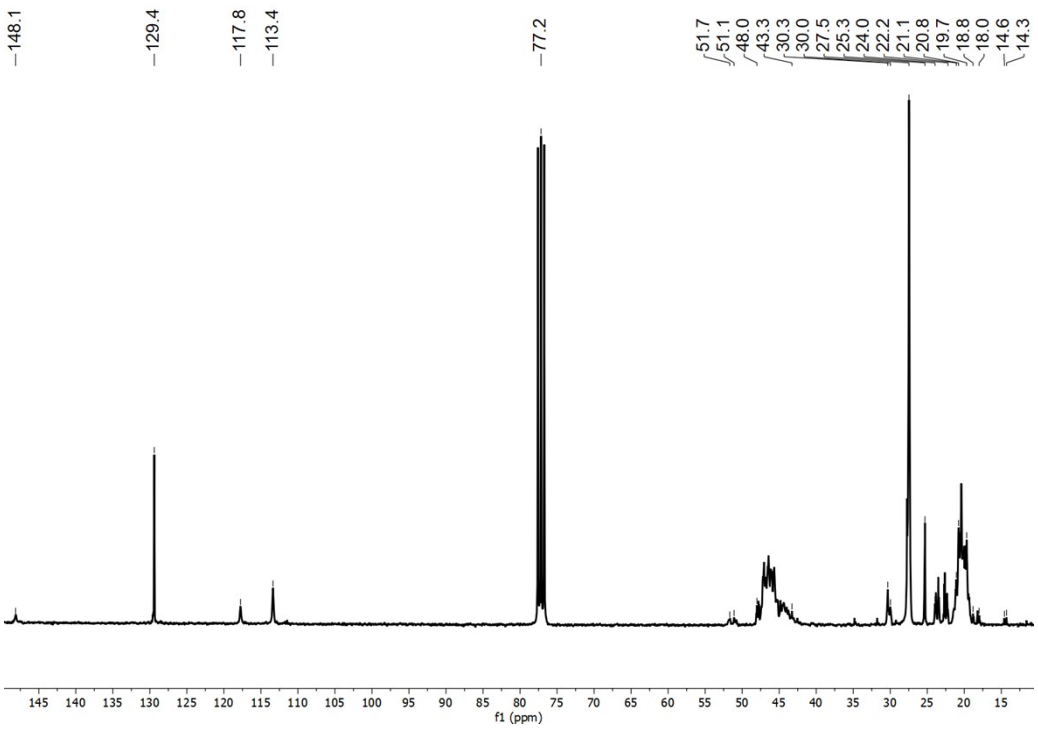

Figure S49. $^{13}C\{^{1}H\}$ NMR spectrum (101 MHz, $CDCl_3$, 298 K) of **AT840-HNMePh**.

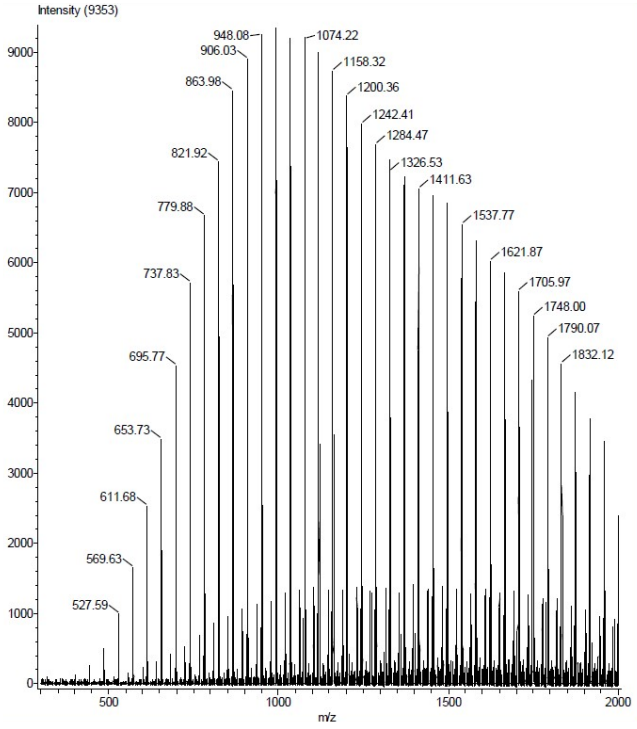

Figure S50. Low resolution field desorption mass spectrum of **AT840-HNMePh**. LRMS (FD) m/z: Calcd for $C_{79}H_{152}N$ 948.86; Found 948.08.

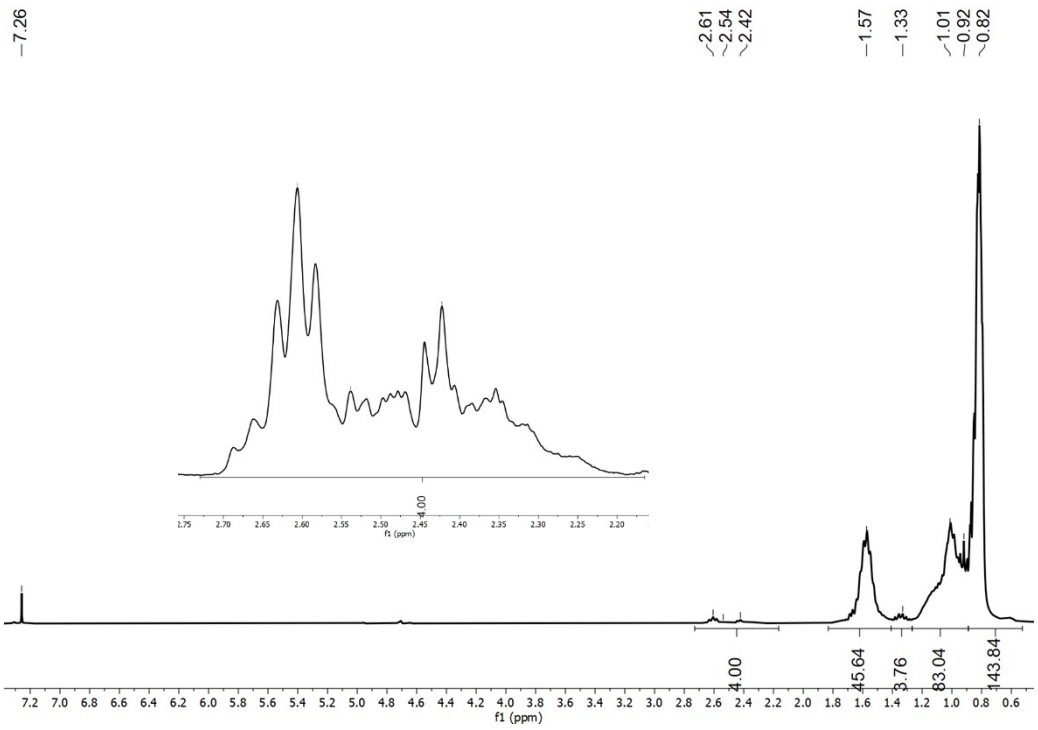

Figure S51. ^{1}H NMR spectrum (300 MHz, $CDCl_3$, 298 K) of **AT840-HNMeBu**.

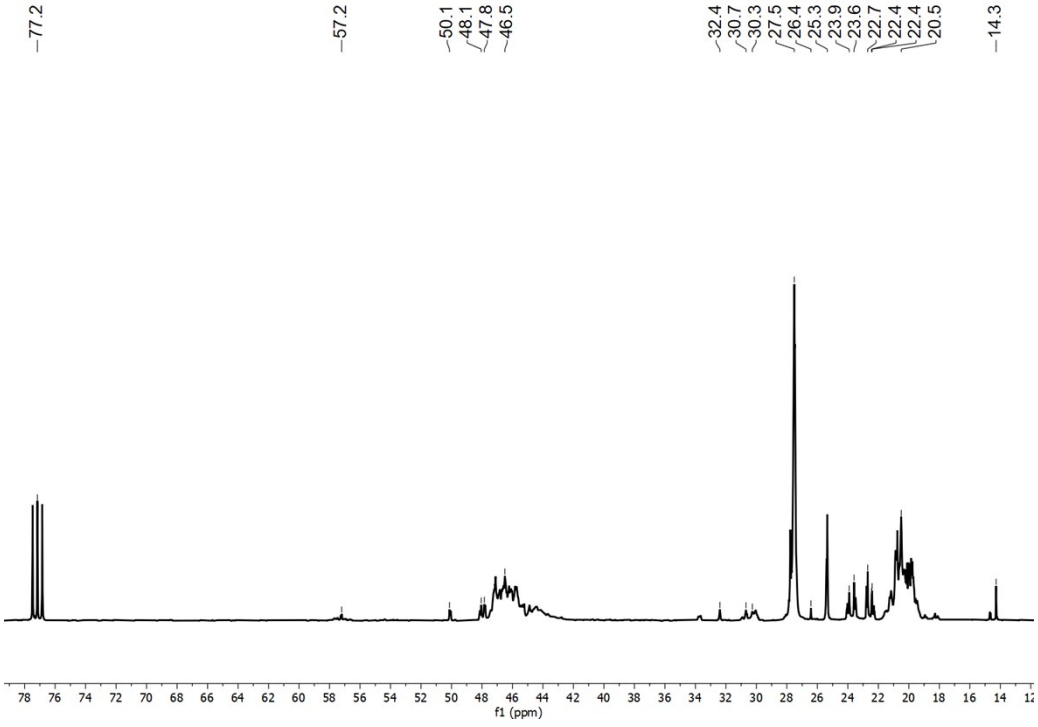

Figure S52. $^{13}C\{^{1}H\}$ NMR spectrum (101 MHz, $CDCl_3$, 298 K) of **AT840-HNMeBu**.

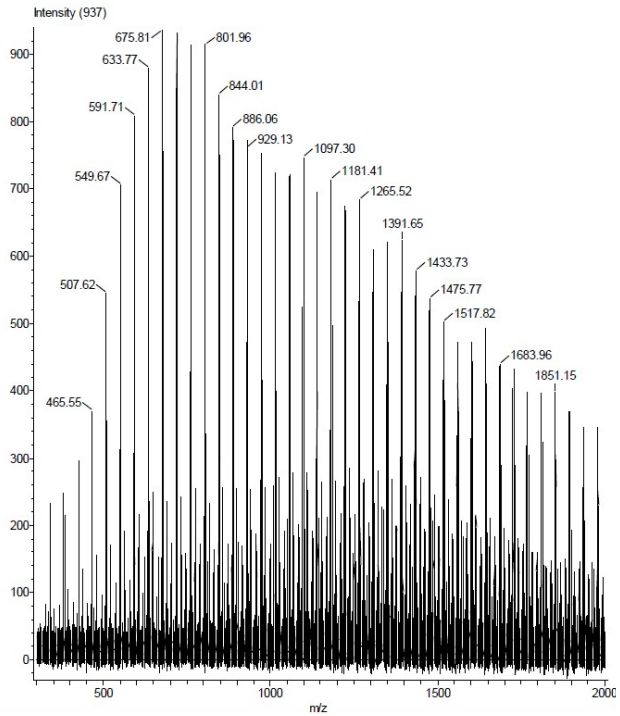

Figure S53. Low resolution field desorption mass spectrum of **AT840-HNMeBu**. LRMS (FD) m/z: Calcd for $C_{77}H_{156}N$ 928.88; Found 929.13.

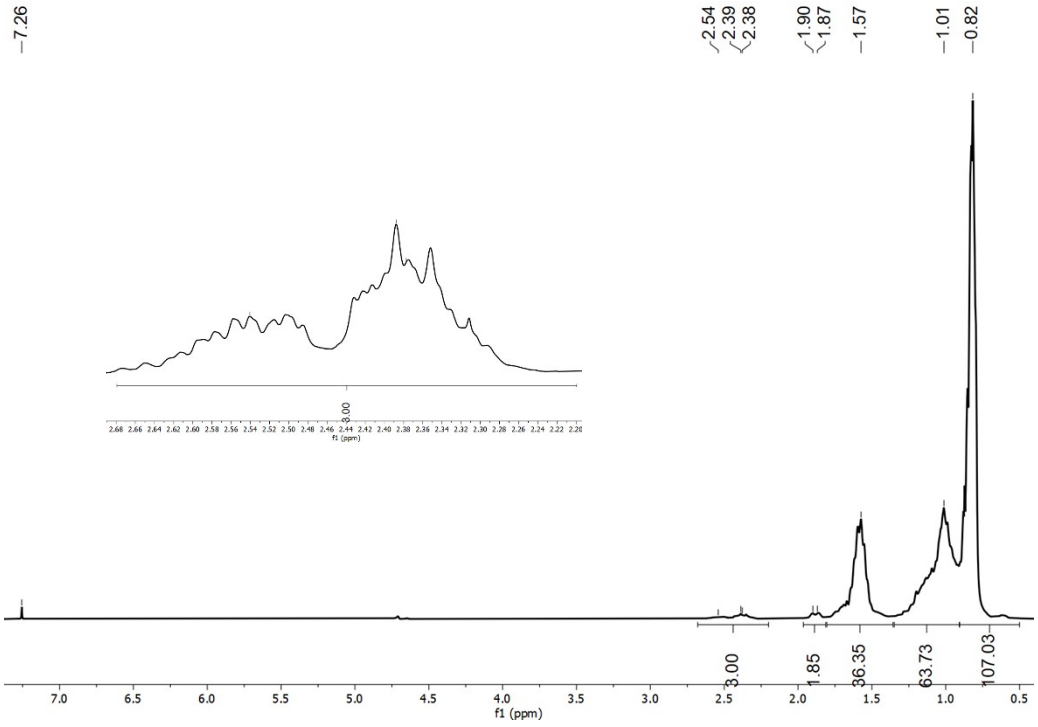

Figure S54. ^{1}H NMR spectrum (300 MHz, $CDCl_3$, 298 K) of **A840-HNMeCy**.

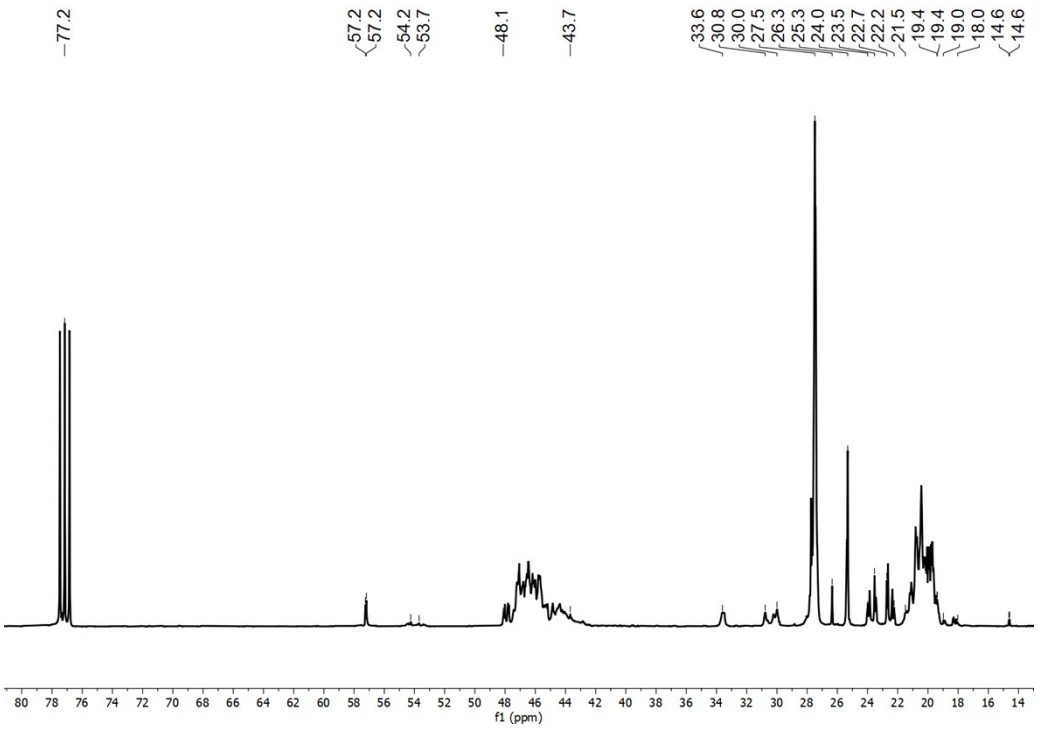

Figure S55. $^{13}C\{^{1}H\}$ NMR spectrum (101 MHz, $CDCl_3$, 298 K) of **AT840-HNMeCy**.

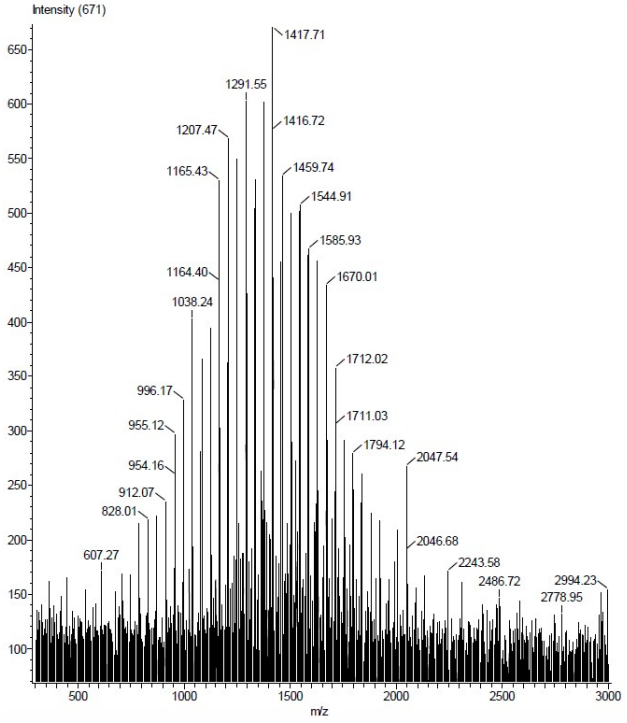

Figure S56. Low resolution field desorption mass spectrum of **AT840-HNMeCy**. LRMS (FD) m/z: Calcd for $C_{79}H_{158}N$ 954.92; Found 955.12.

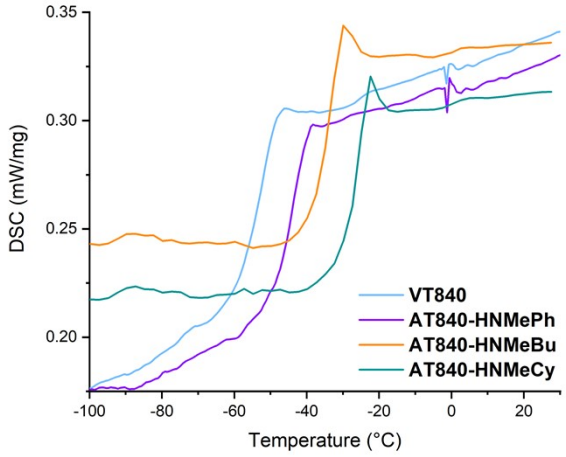

Figure S57. Overlaid DSC thermograms of **VT840** and **AVT840-HNMePh/HNMeBu/HNMeCy**.

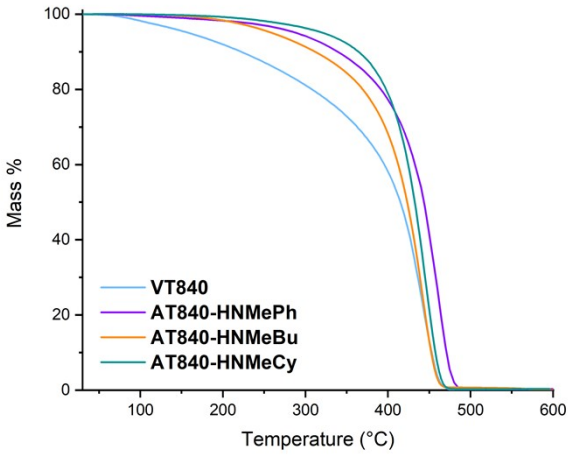

Figure S58. Overlaid TGA thermograms of **VT840** and **AVT840-HNMePh/HNMeBu/HNMeCy**.

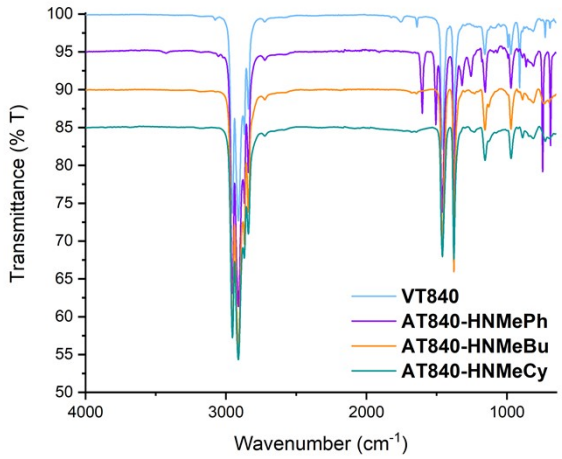

Figure S59. Overlaid IR spectra of **VT840** and aminated analogues **AT840-HNMePh/HNMeBu/HNMeCy**.

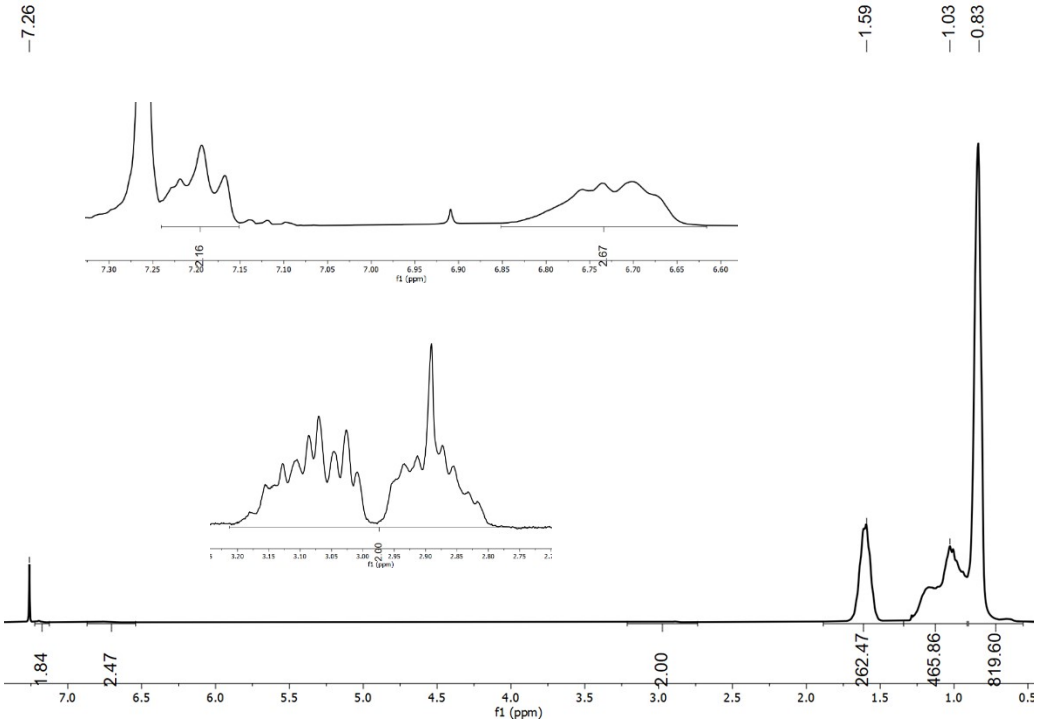

Figure S60. ^{1}H NMR spectrum (300 MHz, $CDCl_3$, 298 K) of **A7200-HNMePh**.

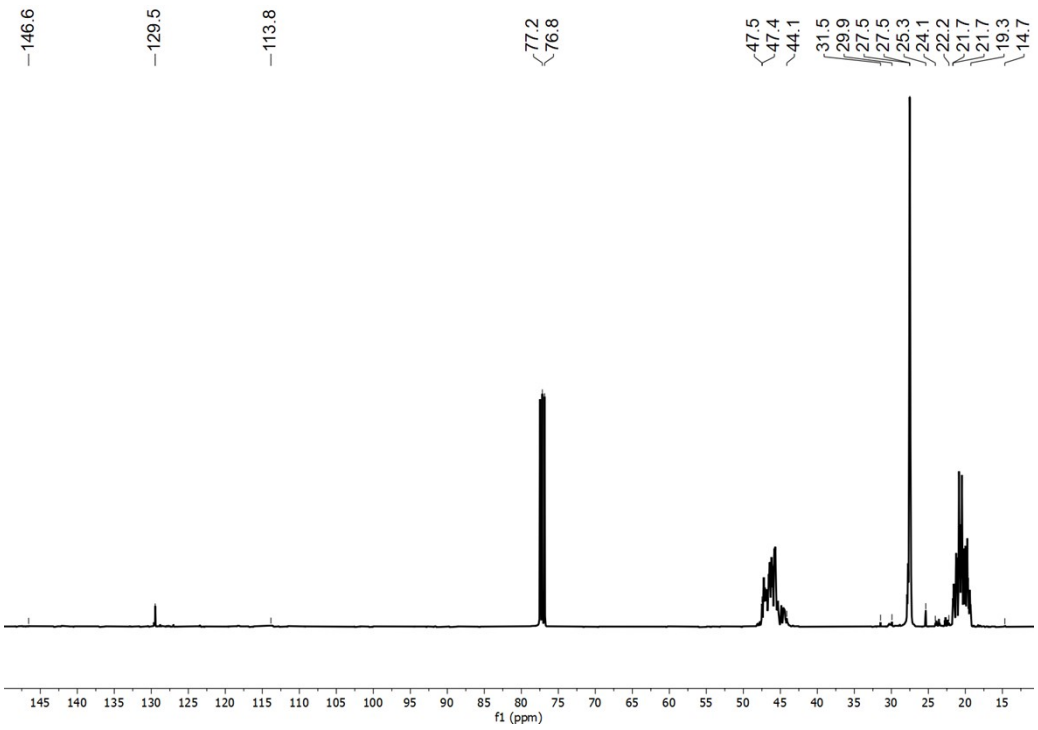

Figure S61. $^{13}C\{^{1}H\}$ NMR spectrum (101 MHz, $CDCl_3$, 298 K) of **A7200-HNMePh**.

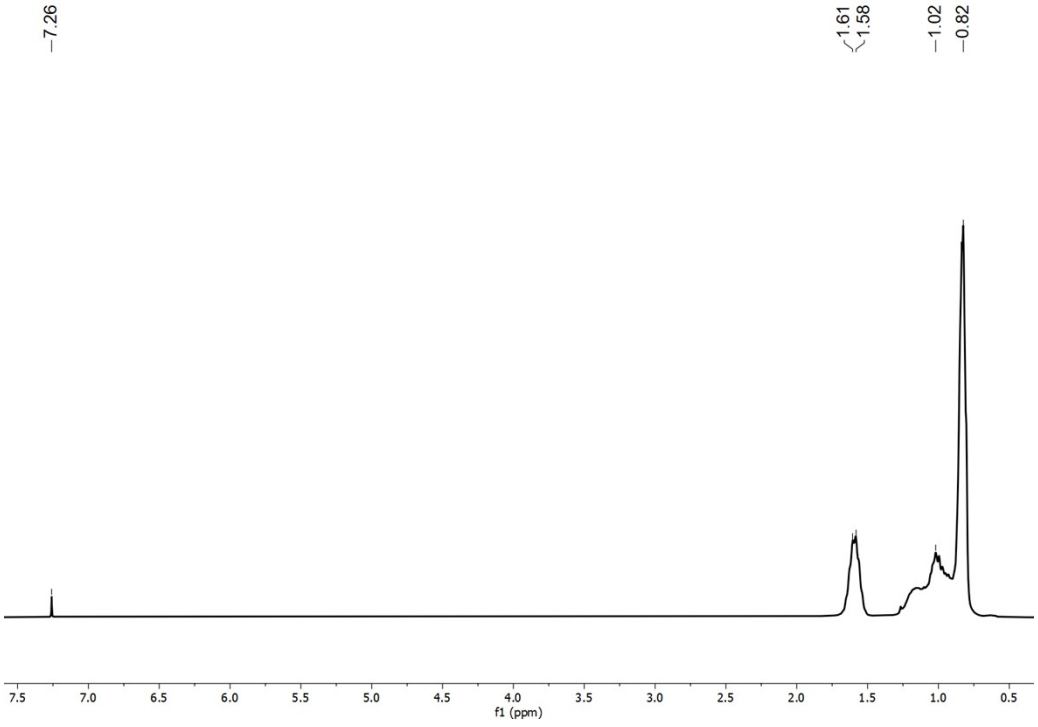

Figure S62. ^{1}H NMR spectrum (300 MHz, $CDCl_3$, 298 K) of **A7200-HNMeBu**.

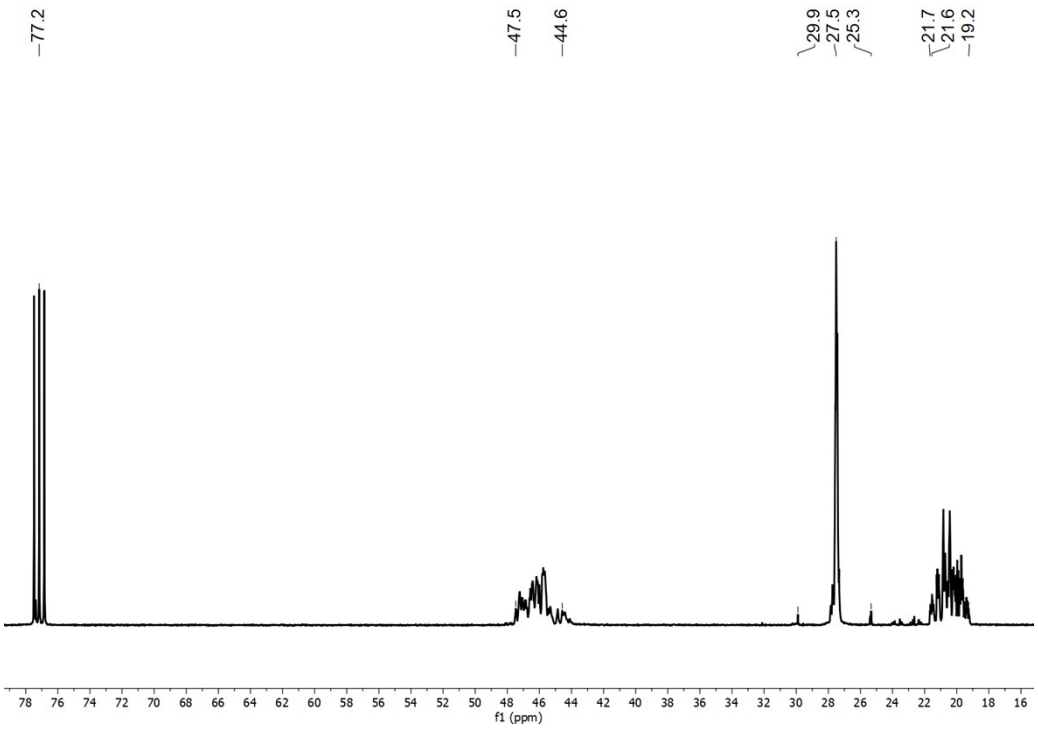

Figure S63. $^{13}C\{^{1}H\}$ NMR spectrum (101 MHz, $CDCl_3$, 298 K) of **A7200-HNMeBu**.

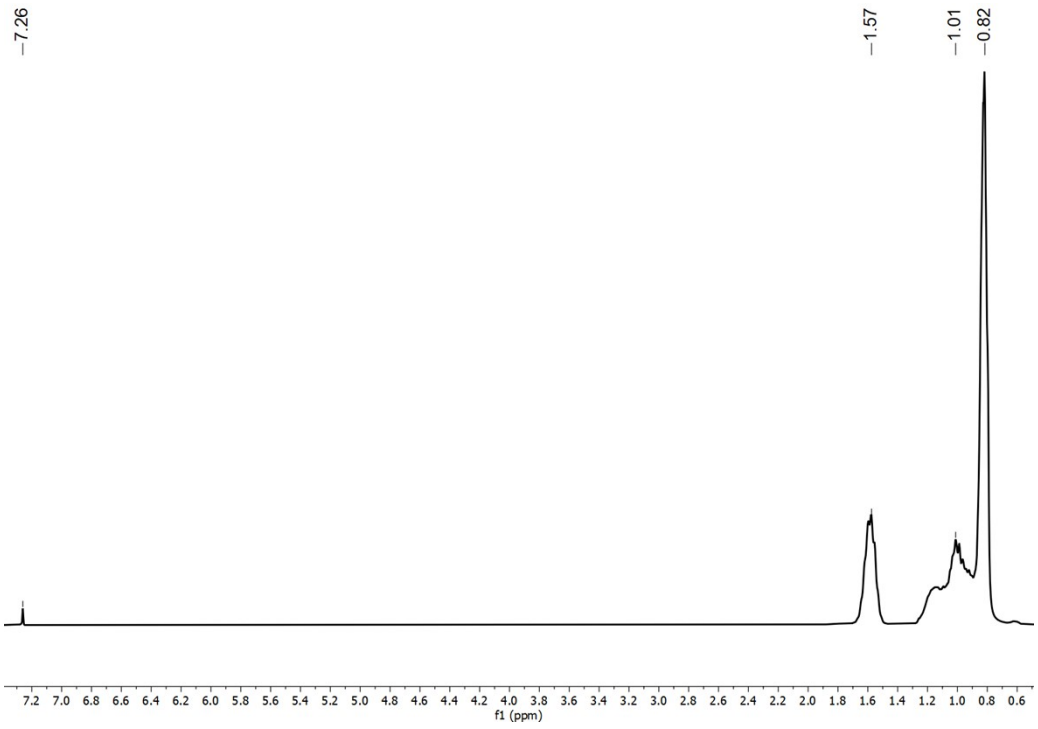

Figure S64. ^{1}H NMR spectrum (300 MHz, $CDCl_3$, 298 K) of **A7200-HNMeCy**.

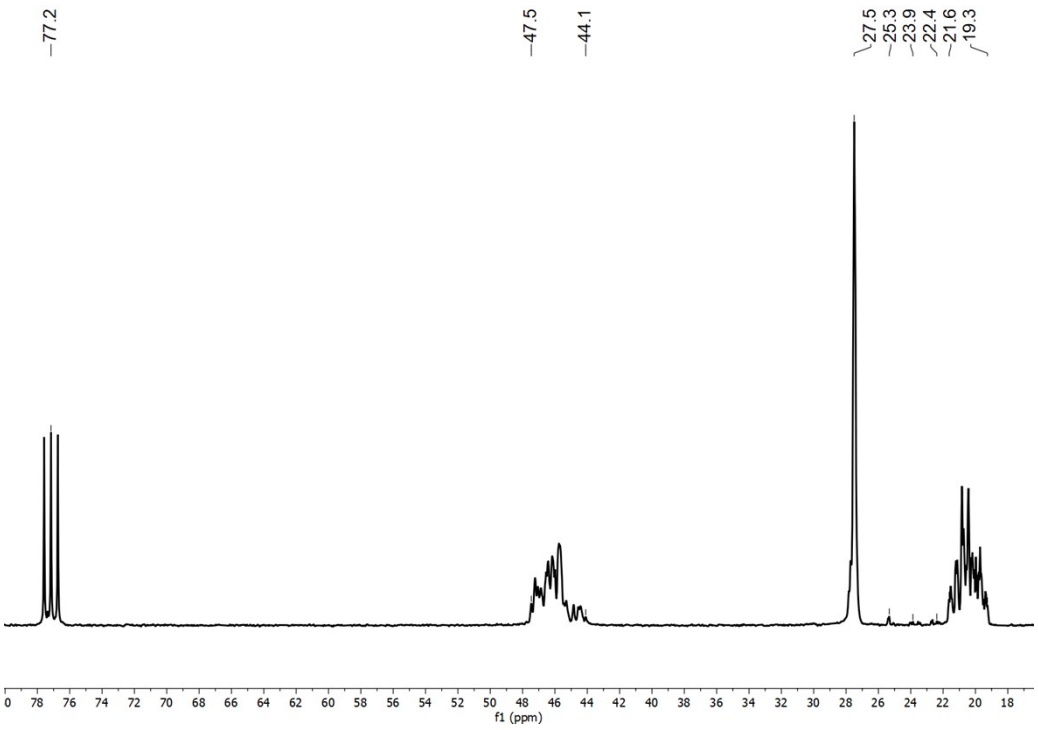

Figure S65. $^{13}C\{^{1}H\}$ NMR spectrum (101 MHz, $CDCl_3$, 298 K) of **A7200-HNMeCy**.

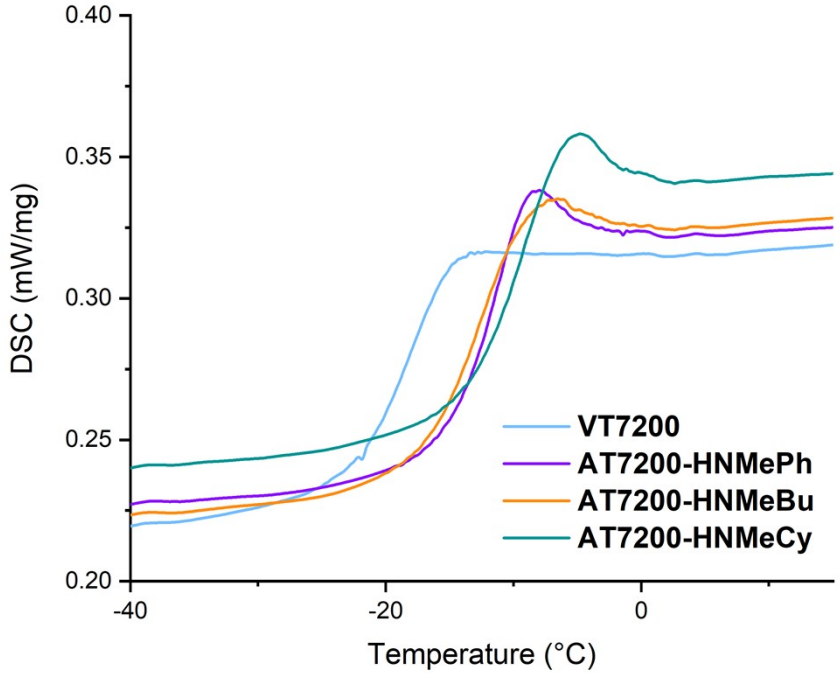

Figure S66. Overlaid DSC thermograms of **VT7200** and **AVT7200-HNMePh/HNMeBu/HNMeCy**.

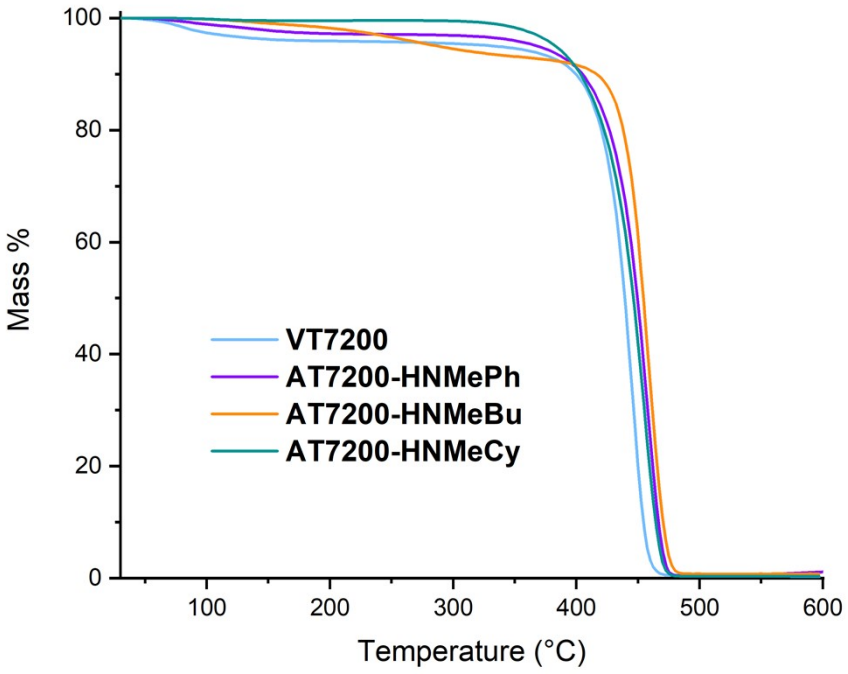

Figure S67. Overlaid TGA thermograms of **VT7200** and **AVT7200-HNMePh/HNMeBu/HNMeCy**.

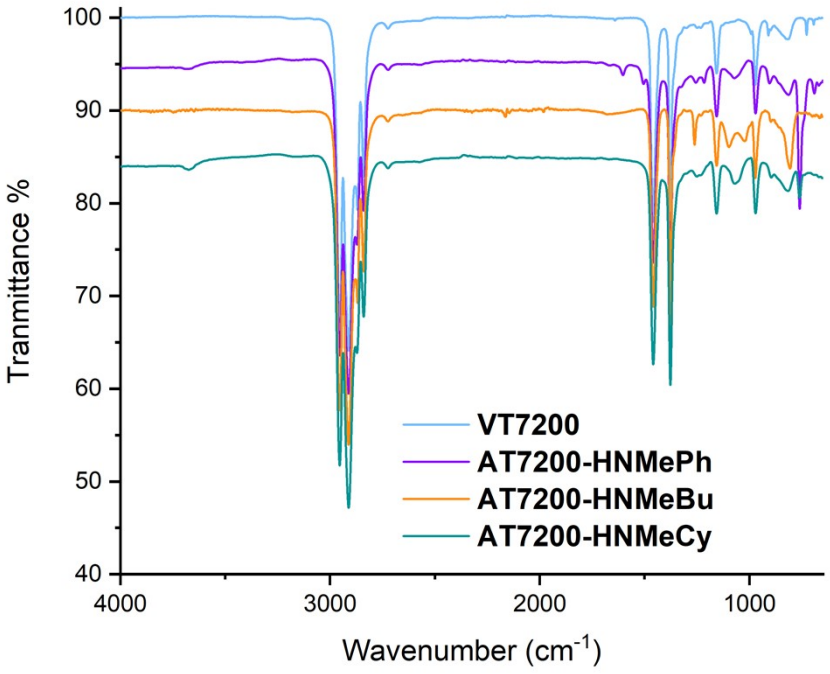

Figure S68. Overlaid IR spectra of **VT7200** and aminated analogues **AT7200-HNMePh/HNMeBu/HNMeCy**.

Table S4. Expected and calculated M_n of ATPP materials based on end-group analysis of the ^1H NMR spectrum and FDMS.

Sample	Expected M_n (g/mol)	M_n (g/mol) by end group analysis	M_n (g/mol) by FDMS
AT230-HNMePh	317.31	392	317.30
AT230-HNMeBu	297.34	446	297.33
AT230-HNMeCy	323.36	383	323.33
AT350-HNMePh	443.45	517	443.47
AT350-HNMeBu	423.48	471	423.57
AT350-HNMeCy	449.50	635	449.50
AT840-HNMePh	948.86	1438	948.08
AT840-HNMeBu	928.88	1981	929.13
AT840-HNMeCy	954.92	1502	955.12
AT7200-HNMePh	7307.17	10965	N/A
AT7200-HNMeBu	7287.19	N/A	N/A
AT7200-HNMeCy	7313.32	N/A	N/A

Table S5. Expanded tabulation of expanded T_g values of VTPP and ATPP materials from DSC thermograms.

Sample	T_g Onest (°C)	T_g Mid (°C)	T_g Inflection (°C)	T_g End (°C)
VT230	-117.2	-115.8	-114.6	-114.3
AT230-HNMePh	-66.1	-63.8	-62.2	-61.0
AT230-HNMeBu	-91.2	-88.7	-88.2	-86.2
AT230-HNMeCy	-78.7	-77.5	-74.7	-75.2
VT350	-84.5	-83.3	-81.7	-81.7
AT350-HNMePh	-52.5	-51.1	-49.0	-49.0
AT350-HNMeBu	-71.6	-69.8	-67.8	-67.2
AT350-HNMeCy	-75.0	-68.3	-68.4	-61.4
VT840	-59.3	-54.3	-50.9	-49.0
AT840-HNMePh	-48.6	-43.6	-43.6	-38.8
AT840-HNMeBu	-43.8	-39.2	-38.1	-35.1
AT840-HNMeCy	-42.9	-35.1	-34.3	-28.7
VT7200	-21.2	-17.7	-17.5	-14.4
AT7200-HNMePh	-13.9	-11.7	-10.6	-9.5
AT7200-HNMeBu	-15.7	-12.5	-11.8	-9.5
AT7200-HNMeCy	-12.5	-9.6	-9.0	-6.8

Table S6. Expanded tabulation of 5%, 50%, and 95% thermal degradation of VTPP and ATPP materials from TGA thermogram.

Sample	5% Weight Loss (°C)	50% Weight Loss (°C)	95% Weight Loss (°C)
VT230	105.8	161.9	189.6
AT230-HNMePh	153.3	234.1	314.7
AT230-HNMeBu	154.9	236.8	418.7
AT230-HNMeCy	157.4	233.7	280.5
VT350	179.9	246.4	275.9
AT350-HNMePh	233.7	313.3	341.2
AT350-HNMeBu	197.5	271.4	332.6
AT350-HNMeCy	224.2	302.4	349.8
VT840	158.9	415.0	458.2
AT840-HNMePh	230.9	423.1	458.9
AT840-HNMeBu	259.6	423.2	457.1
AT840-HNMeCy	321.5	432.4	461.7
VT7200	333.8	439.2	457.9
AT7200-HNMePh	368.3	449.5	469.8
AT7200-HNMeBu	287.2	454.3	473.9
AT7200-HNMeCy	383.1	446.2	467.7

S4. Life Cycle Analysis

The life cycle analysis (LCA) was performed following a published procedure[3] for the synthesis of *N*-(2-methyloctyl)aniline using either the titanium catalyst[4] or the tantalum catalyst supported by the cyclic ureate ligand published in 2020 by our group[5] with an updated ligand synthesis published in 2022.[6] This analysis is gate-to-gate, meaning the synthesis of the commercially available precursors was not considered, nor the impact of the of the final product, *N*-(2-methyloctyl)aniline. The masses of the reagents used in the pre-catalyst and ligand synthesis were based on experimentally obtained yields to achieve 5 mol% of each ligand and metal complex with respect to the 1-octene and *N*-methylaniline reagents. The concentrations of solutions were based on reported amounts of solvents used in small scale reactions reported (Ta: 0.867 $mol_{reagent}/L_{tol}$, Ti: 1 $mol_{reagent}/L_{tol}$) and catalytic reactivity was assumed to be transferable to the 1 kg scale. It was assumed that *N*-(2-methyloctyl)aniline would form quantitatively from the hydroaminoalkylation reaction between 1-octene and *N*-methylaniline with each catalyst based on reported results and experimentally obtained results within our lab. The product was assumed to be isolated by distillation in both methods, therefore a net difference of zero for CO_2 energy byproduct in distillation was assumed and does not contribute to the final calculation. Drying agents for solvents (calcium hydride for dichloromethane, sodium for tetrahydrofuran, and SPS drying columns for toluene and hexanes) were not considered because these can be reused to reduce their environmental impact to negligible amounts over their lifetimes. Metal waste is assumed to escape 100% to the environment and organic waste is assumed to be incinerated with only 0.1% escape to the environment. To this, transition metal catalyst precursors were assumed to escape 100% to the environment while the supporting *N*,*O*-chelating ligand was addressed separately and assumed to escape only 0.1%. The syntheses in the tantalum-catalyzed route are multi-step where the conversion to the intermediate is not quantitative. In these cases, the difference between the moles of the isolated product and the intermediate product are used to determine the mass emitted of intermediate products. The procedure does not take into account the energy required to cool, pressurize gases, or maintain an air-free environment (i.e. glovebox power usage or vacuum pump for Schlenk line). To this, if these aspects were accounted for the tantalum-catalyzed synthesis would be substantially more energy demanding, consequently producing substantially more CO_2 than the titanium-catalyzed route. The CO_2 energy byproduct for solvent heating, evaporating, and refluxing was reported based on Mercer et al. The tantalum catalyzed hydroaminoalkylation was considered a refluxing reaction (110 °C) and the titanium-catalyzed reaction was considered as heating the solvent (160 °C). The reaction times used for the reflux energy CO_2 production calculation was 1 h for the tantalum-catalyzed reaction based on experimentally obtained results and 2 h for the titanium-catalyzed reactions, these were based on reported literature procedures. LD50 values obtained were for oral rat and LC50 values were for 4 h inhalation from chemical supplier SDS, and were used for the INGTP and INHTP calculations, unless otherwise stated. Henry's law constant values and log K_{ow} values were obtained from predictions reported by chemspider.com, unless otherwise stated. All soil sorption coefficient (K_{oc}) was estimated by $K_{oc} = K_{ow}(0.41)$, except for magnesium(0) turnings which K_{oc} was obtained from prediction reported by chemspider.com.

The following are reagent specific assumptions made in creating the LCA:

- The solvent “hexanes” was assessed as n-hexane
- Maximum Incremental Reactivity (MIR) values:[7-10]
    - *N*-methylaniline was estimated by ethylbenzene
    - 2,6-diisopropylaniline was estimated by 1,3-diisopropylbenzene
- LC50:
    - *N*-methylaniline: value provided for water flea 48 h
    - *Bis*(trimethylsilyl)amine value provided for 6 h
- Boethling numbers:[11]
    - Triphosgene: estimated by 1 ester and 1 ether since carbonate is not available
    - 2-imidazolidone: estimated by 1 amide and 1 aliphatic amine since urea is not available
    - 1,3-di-tert-butylimidazolidin-2-one: estimated by 1 amide and 1 tertirary amine since urea is not available
    - 1-(tert-butyl)imidazolidin-2-one: estimated by 1 amide and 1 aliphatic amine since urea is not available
    - 1-(tert-butyl)-4,5-dihydro-1H-imidazol-2-olate: estimated by 1 amide since ureate is not available
    - All other reagents with functional groups not provided by Boethling et al. were not estimated and not considered
- Henry’s Law constant:
    - Magnesium(II) bromide was estimated to be 0
    - Magnesium(II) chloride was estimated to be 0
    - *Bis*[(trimethyl)silylmethyl]zinc(II) was estimated to be 0
    - Tantalum(V) chloride was estimated to be 0
    - *Tris*[(trimethyl)silylmethyl]tantalum(V) chloride was estimated to be 0
    - *Tetrakis*(dimethylamido)titanium(IV) was estimated to be 0
- CO_2 produced by energy consumption during the heating of the tantalum-catalyzed hydroaminoalkylation reaction was treated as a reflux with $T_{b,tol}$ = 383.75 K.
- CO_2 produced by energy consumption during the heating of the titanium-catalyzed hydroaminoalkylation reaction was treated as heating the liquid to 433.15 K, based on reported reaction conditions.

The E Factor (EF)[12] was calculated using equation 1 and the reaction mass efficiency (RME)[3] was calculated using equation 2.

$$EF = \frac{mass\ of\ waste\ (kg)}{mass\ of\ product\ (kg)} = \frac{\sum mass\ of\ reagents\ for\ catalyst\ synthesis\ (kg) + \sum mass\ of\ all\ solvents\ (kg)}{mass\ of\ product\ (kg)} \quad (Eq\ 1)$$

$$RME = \frac{mol\ wt\ product}{\sum mol\ wt\ reactants\ (including\ catalyst)} \times 100\% \quad (Eq\ 2)$$

Table S7. Materials for tantalum-catalyzed hydroaminoalkylation for 1 g synthesis of *N*-(2-methyloctyl)aniline. Masses used and emitted rounded to the nearest whole number.

Chemical Name	Role	Mass Used (g)	Mass Produced (g)	Mass Emitted (g)
magnesium(0) turnings	reagent	121	--	--
1,2-dibromoethane	reagent	154	--	--
(chloromethyl)trimethylsilane	reagent	390	--	--
ethylene	byproduct	--	23	23
magnesium(II) bromide	byproduct	--	151	151
((trimethylsilyl)methyl)magnesium(II) chloride	product/reagent	467	467	--
zinc(II) chloride	reagent	217	--	--
magnesium(II) chloride	byproduct	--	303	303
bis[(trimethylsilyl)methyl]zinc(II)	product/reagent	99	380	281
tantalum(V) chloride	reagent	93	--	11
zinc(II) chloride	byproduct	--	57	57
(bis(trimethylsilyl)methyl)tantalum(V) chloride	product/reagent	117	117	117
tetrahydrofuran	solvent	956	--	0.956
hexanes	solvent	159	--	0.159
2-imidazolidone	reagent/byproduct	47	5	0.005
1,3-di-tert-butylimidazolidin-2-one	byproduct	--	32	0.032
1-(tert-butyl)imidazolidin-2-one	product	46	46	2.9E-05
tert-butanol	reagent	41	--	0.041
sulfuric acid	reagent	117	--	117
sodium bis(trimethylsilyl)amide	reagent	60	--	0.0017
bis(trimethylsilyl)amine	byproduct	--	16	0.016
1-(tert-butyl)-4,5-dihydro-1H-imidazol-2-olate	product	37	--	0.037
hexanes	solvent	70	--	0.070
toluene	solvent	138	--	0.138
1-octene	reagent	512	--	0.512
N-methylaniline	reagent	488	--	0.488

toluene	solvent	4558	--	4.558
carbon dioxide	energy byproduct	--	70528	70528

Table S8. Potentials for synthesis of tantalum-catalyzed hydroaminoalkylation to form *N*-(2-methyloctyl)aniline.

Chemical Name	AP	ODP	SFP	GWP	INGTP	INHTP	PER	ACCU Log K_{ow}	ADP
magnesium(0) turnings	**--**	**--**	**--**	**--**	**N/A**	**--**	**weeks**	**-5.70E-01**	3.73E-09
1,2-dibromoethane	**--**	**--**	**--**	**--**	**--**	**--**	**months**	**2.08E+00**	1.33E-02
(chloromethyl)trimethylsilane	**--**	**--**	**N/A**	**--**	**N/A**	**N/A**	**months**	**2.52E+00**	4.86E-08
ethylene	**--**	**--**	**5.49E+01**	**7.21E+01**	**3.91E+01**	**N/A**	**weeks**	**1.32E+00**	1.00E-06
magnesium(II) bromide	**--**	**--**	**N/A**	**--**	**--**	**--**	**months**	**N/A**	6.67E-03
((trimethylsilyl)methyl)magnesium(II) chloride	**--**	**--**	**N/A**	**--**	**--**	**--**	**months**	**2.17E+00**	5.23E-08
zinc(II) chloride	**--**	**--**	**N/A**	**--**	**--**	**--**	**months**	**1.50E-01**	9.92E-04
magnesium(II) chloride	**--**	**--**	**N/A**	**--**	**--**	**--**	**months**	**N/A**	1.01E-07
***bis*[(trimethylsilyl)methyl]zinc(II)**	**--**	**--**	**N/A**	**4.12E+02**	**--**	**--**	**months**	**N/A**	9.92E-04
tantalum(V) chloride	**--**	**--**	**N/A**	**--**	**--**	**--**	**months**	**N/A**	6.79E-05
zinc(II) chloride	**--**	**--**	**N/A**	**--**	**1.91E+05**	**--**	**months**	**1.50E-01**	9.92E-04
(*bis*(trimethylsilyl)methyl)tantalum(V) chloride	**--**	**--**	**N/A**	**1.20E+02**	**--**	**--**	**months**	**N/A**	6.78E-05
tetrahydrofuran	**--**	**--**	**1.53E+00**	**2.27E+00**	**3.26E+01**	**3.12E-01**	**weeks**	**3.30E-01**	1.00E-06
hexanes	**--**	**--**	**5.01E-02**	**4.85E-01**	**2.57E-02**	**1.36E-02**	**weeks**	**3.94E+00**	1.00E-06
2-imidazolidone	--	--	--	7.17E-03	-1.22E-03	N/A	months	-1.23E+00	1.00E-06
1,3-di-tert-butylimidazolidin-2-one	--	--	--	7.92E-02	N/A	N/A	months	2.43E+00	1.00E-06
1-(tert-butyl)imidazolidin-2-one	--	--	--	6.26E-05	N/A	N/A	months	8.10E-01	1.00E-06
tert-butanol	--	--	5.57E-03	9.77E-02	5.48E-01	N/A	weeks	5.10E-01	1.00E-06
sulfuric acid	6.54E-01	--	--	--	-7.46E+05	--	months	-1.03E+00	3.58E-04
sodium *bis*(trimethylsilyl)amide	--	--	--	2.44E-03	N/A	N/A	months	N/A	1.00E-06
bis(trimethylsilyl)amine	--	--	N/A	2.59E-02	4.32E+03	1.45E+01	months	2.32E+00	1.00E-06
1-(tert-butyl)-4,5-dihydro-1H-imidazol-2-olate	--	--	--	7.02E-02	N/A	N/A	months	N/A	1.00E-06
hexanes	--	--	2.20E-02	2.13E-01	1.13E-02	5.98E-03	weeks	3.94E+00	1.00E-06

toluene	--	--	1.20E-01	4.62E-01	1.38E-01	1.38E-01	weeks	2.68E+00	1.00E-06
1-octene	--	--	4.46E-01	1.60E+00	3.41E-01	2.55E+01	weeks	3.68E+00	1.00E-06
N-methylaniline	--	--	4.79E-01	1.40E+00	1.09E+01	2.84E-01	months	1.60E+00	1.00E-06
toluene	--	--	3.97E+00	1.52E+01	4.56E+00	4.56E+00	weeks	2.68E+00	1.00E-06
carbon dioxide	--	--	N/A	7.05E+04	N/A	2.85E+03	N/A	8.30E-01	1.00E-06

Table S9. Table of Indices for synthesis of tantalum-catalyzed hydroaminoalkylation. Bolded entries are part of tantalum precursor synthesis. Non-bolded entries are part of the catalyst ligand synthesis. Entries with grey text represent reagents and solvents used in catalytic reaction. Impact for total calculated CO_2 production from energy consumption in blue font. For columns I_{AP} to I_{INHT} the worst performing aspect of the synthesis has been highlighted red. PER is coded where weeks = yellow, months = orange, very long-lived = red to visually indicate their impact. ACCU is coded where green < 3.5, yellow = 3.5-4.3, and red >4.3, to visually indicate boundaries for relative impact of each value. I_{AD} has been coded to represent the 1-octene and *N*-methylaniline as red with more depleting reagents being darker shades of red. Values of zero are represented at "--" and values that could not be obtained are listed as "N/A".

Chemical Name	I_{AP}/g	I_{OD}/g	I_{SF}/g	I_{GW}/g	I_{INGT}/g	I_{INHT}/g	PER	ACCU Log K_{ow}	I_{AD}/g
magnesium(0) turnings	**--**	**--**	**--**	**--**	**N/A**	**--**	**weeks**	**-5.70E-01**	**--**
1,2-dibromoethane	**--**	**--**	**--**	**--**	**--**	**--**	**months**	**2.08E+00**	**2.06E+00**
(chloromethyl)trimethylsilane	**--**	**--**	**N/A**	**--**	**N/A**	**N/A**	**months**	**2.52E+00**	**1.89E-05**
ethylene	**--**	**--**	**5.49E+01**	**7.21E+01**	**3.91E+01**	**N/A**	**weeks**	**1.32E+00**	**--**
magnesium(II) bromide	**--**	**--**	**--**	**--**	**--**	**--**	**months**	**N/A**	**--**
((trimethylsilyl)methyl)magnesium(II) chloride	**--**	**--**	**N/A**	**--**	**--**	**--**	**months**	**2.17E+00**	**2.45E-05**
zinc(II) chloride	**--**	**--**	**--**	**--**	**--**	**--**	**months**	**1.50E-01**	**2.15E-01**
magnesium(II) chloride	**--**	**--**	**--**	**--**	**--**	**--**	**months**	**N/A**	**--**
***bis*[(trimethylsilyl)methyl]zinc(II)**	**--**	**--**	**N/A**	**4.12E+02**	**--**	**--**	**months**	**N/A**	**9.87E-02**
tantalum(V) chloride	**--**	**--**	**--**	**--**	**--**	**--**	**months**	**N/A**	**6.31E-03**
zinc(II) chloride	**--**	**--**	**--**	**--**	**1.91E+05**	**--**	**months**	**1.50E-01**	**--**
(*bis*(trimethylsilyl)methyl)tantalum(V) chloride	**--**	**--**	**N/A**	**1.20E+02**	**--**	**--**	**months**	**N/A**	**7.93E-03**
tetrahydrofuran	**--**	**--**	**1.53E+00**	**2.27E+00**	**3.26E+01**	**3.12E-01**	**weeks**	**3.30E-01**	**9.56E-04**
hexanes	**--**	**--**	**5.01E-02**	**4.85E-01**	**2.57E-02**	**1.36E-02**	**weeks**	**3.94E+00**	**1.59E-04**
2-imidazolidone	--	--	N/A	7.17E-03	-1.22E-03	N/A	months	-1.23E+00	4.68E-05
1,3-di-tert-butylimidazolidin-2-one	--	--	N/A	7.92E-02	N/A	N/A	months	2.43E+00	--

1-(tert-butyl)imidazolidin-2-one	--	--	N/A	6.26E-05	N/A	N/A	months	8.10E-01	4.62E-05
tert-butanol	--	--	5.57E-03	9.77E-02	5.48E-01	N/A	weeks	5.10E-01	4.11E-05
sulfuric acid	7.64E+01	--	--	--	-7.46E+05	--	months	-1.03E+00	4.19E-02
sodium *bis*(trimethylsilyl)amide	--	--	N/A	2.44E-03	N/A	N/A	months	N/A	5.96E-05
bis(trimethylsilyl)amine	--	--	N/A	2.59E-02	4.32E+03	1.45E+01	months	2.32E+00	--
1-(tert-butyl)-4,5-dihydro-1H-imidazol-2-olate	--	--	N/A	7.02E-02	N/A	N/A	months	N/A	3.74E-05
hexanes	--	--	2.20E-02	2.13E-01	1.13E-02	5.98E-03	weeks	3.94E+00	6.96E-05
toluene	--	--	1.20E-01	4.62E-01	1.38E-01	1.38E-01	weeks	2.68E+00	1.38E-04
1-octene	--	--	4.46E-01	1.60E+00	3.41E-01	2.55E+01	weeks	3.68E+00	5.12E-04
N-methylaniline	--	--	4.79E-01	1.40E+00	1.09E+01	2.84E-01	months	1.60E+00	4.88E-04
toluene	--	--	3.97E+00	1.52E+01	4.56E+00	4.56E+00	weeks	2.68E+00	4.56E-03
carbon dioxide	--	--	N/A	7.05E+04	N/A	2.85E+03	N/A	8.30E-01	--
sum	7.64E+01	--	6.15E+01	7.12E+04	-5.51E+05	2.89E+03	months	3.94E+00	2.43E+00
carbon dioxide production (kg)	70.5								
Reaction Mass Efficiency (RME)	44.65								
E factor (EF)	7.12								

Table S10. Materials for titanium-catalyzed hydroaminoalkylation for 1 g synthesis of *N*-(2-methyloctyl)aniline. Masses used and emitted rounded to the nearest whole number.

Chemical Name	Role	Mass Used (g)	Mass Produced (g)	Mass Emitted (g)
tetrakis(dimethylamido)titanium	**reagent**	**51**	**--**	**51**
diisopropylaniline	reagent	46	--	0.0058
triphosgene	reagent	26	--	0.0094
hydrochloric acid	byproduct	--	19	19
N-methyl-1-phenylethan-1-amine	reagent	35	--	0.034
diisopropylethylamine	reagent	101	101	0.101
dichloromethane	solvent	1370	--	1.370
ethylacetate	solvent	127	--	0.127

hydrochloric acid	reagent	19	--	19
3-(2,6-diisopropylphenyl)-1-methyl-1-(1-phenylethyl)urea (L1)	product/reagent	77	77	0.077
1-octene	reagent	512	--	0.512
N-methylaniline	reagent	488	--	0.488
toluene	solvent	3952	--	1.582
Carbon dioxide	energy byproduct	--	53110	53110

Table S11. Potentials for synthesis of titanium-catalyzed hydroaminoalkylation to form *N*-(2-methyloctyl)aniline.

Chemical Name	AP	ODP	SFP	GWP	INGTP	INHTP	PER	ACCU Log K_{ow}	ADP
tetrakis(dimethylamido)titanium	**--**	**--**	**N/A**	**1.57E+00**	**--**	**--**	**months**	**-2.56E-01**	**4.40E-08**
diisopropylaniline	--	--	1.77E+00	2.98E+00	6.72E+02	N/A	months	3.61E+00	1.00E-06
triphosgene	--	--	N/A	4.45E-01	5.78E+02	5.42E+01	very long-lived	4.02E+00	1.458E-07
hydrochloric acid	0.879046	--	N/A	--	1.24E+08	3.82E-06	weeks	--	4.86E-08
N-methyl-1-phenylethan-1-amine	--	--	N/A	2.93E+00	N/A	N/A	months	1.87E+00	1.00E-06
diisopropylethylamine	--	--	N/A	2.72E+00	1.43E+04	3.24E-01	months	2.35E+00	1.00E-06
dichloromethane	--	--	1.29E-01	5.18E-01	5.45E+03	7.87E-01	months	1.19E+00	9.72E-08
ethylacetate	--	--	2.03E-01	2.00E+00	3.91E+03	--	weeks	7.10E-01	1.00E-06
hydrochloric acid	0.879046	--	N/A	--	1.24E+08	3.82E-06	weeks	--	4.86E-08
3-(2,6-diisopropylphenyl)-1-methyl-1-(1-phenylethyl)urea (L1)	--	--	N/A	2.86E+00	--	--	months	N/A	1.00E-06
1-octene	--	--	8.71E-01	3.14E+00	6.67E+02	4.98E+01	weeks	3.68E+00	1.00E-06
N-methylaniline	--	--	9.81E-01	2.87E+00	2.23E+04	5.82E-01	months	1.60E+00	1.00E-06
toluene	--	--	8.71E-01	3.34E+00	1.00E+03	1.00E+00	weeks	2.68E+00	1.00E-06

Carbon dioxide	--	--	--	1.00E+00	N/A	2.85E+03	weeks	8.30E-01	1.00E-06

Table S12. Table of Indices for synthesis of titanium-catalyzed hydroaminoalkylation. Bolded entries are part of tantalum precursor synthesis. Non-bolded entries are part of the catalyst ligand synthesis. Entries with grey text represent reagents and solvents used in catalytic reaction. Impact for total calculated CO_2 production from energy consumption in blue font. For columns I_{AP} to I_{INHT} the worst performing aspect of the synthesis has been highlighted red. PER is coded where weeks = yellow, months = orange, very long-lived = red to visually indicate their impact. ACCU is coded where green < 3.5, yellow = 3.5-4.3, and red >4.3, to visually indicate boundaries for relative impact of each value. I_{AD} has been coded to represent the 1-octene and *N*-methylaniline as red with more depleting reagents being darker shades of red. Values of zero are represented at "--" and values that could not be obtained are listed as "N/A".

Chemical Name	I_{AP}/g	I_{OD}/g	I_{SF}/g	I_{GW}/g	I_{INGT}/g	I_{INHT}/g	PER	ACCU Log K_{ow}	I_{AD}/g
tetrakis(dimethylamido)titanium	**--**	**--**	**N/A**	**8.02E+01**	**--**	**--**	**months**	**-2.56E-01**	**2.25E-06**
diisopropylaniline	--	--	1.03E-02	1.73E-02	3.91E+00	N/A	months	3.61E+00	4.62E-05
triphosgene	--	--	N/A	4.19E-03	5.44E+00	5.11E-01	very long-lived	4.02E+00	3.74E-06
hydrochloric acid	1.66E+01	--	N/A	--	2.34E+09	3.82E-06	weeks	--	--
N-methyl-1-phenylethan-1-amine	--	--	N/A	9.85E-02	N/A	N/A	months	1.87E+00	3.51E-05
diisopropylethylamine	--	--	N/A	2.76E-01	1.45E+03	3.28E-02	months	2.35E+00	1.01E-04
dichloromethane	--	--	1.77E-01	7.09E-01	7.46E+03	1.08E+00	months	1.19E+00	1.33E-04
ethylacetate	--	--	2.57E-02	2.53E-01	4.96E+02	--	weeks	7.10E-01	1.27E-04
hydrochloric acid	1.69E+01	--	N/A	--	2.37E+09	7.35E-05	weeks	--	--
3-(2,6-diisopropylphenyl)-1-methyl-1-(1-phenylethyl)urea (L1)	--	--	N/A	2.21E-01	--	--	months	N/A	7.71E-05
1-octene	--	--	4.46E-01	1.60E+00	3.41E+02	2.55E+01	weeks	3.68E+00	5.12E-04
N-methylaniline	--	--	4.79E-01	1.40E+00	1.09E+04	2.84E-01	months	1.60E+00	4.88E-04
toluene	--	--	3.44E+00	1.32E+01	3.95E+03	3.95E+00	weeks	2.68E+00	3.95E-03
Carbon dioxide	--	--	--	5.31E+04	N/A	2.85E+03	weeks	8.30E-01	--
sum	3.35E+01	--	4.58E+00	9.80E+01	4.71E+09	3.13E+01	very long-lived	4.02E+00	5.48E-03

Carbon dioxide production (kg)	53.1
Reaction Mass Efficiency (RME)	79.39
E Factor (EF)	6.73

S5. Literature

1. Majer, P.; Randad, R. S., A Safe and Efficient Method for Preparation of N,N'-Unsymmetrically Disubstituted Ureas Utilizing Triphosgene. *The Journal of Organic Chemistry* **1994**, *59* (7), 1937-1938.
2. Edwards, P. M.; Schafer, L. L., In Situ Generation of a Regio- and Diastereoselective Hydroaminoalkylation Catalyst Using Commercially Available Starting Materials. *Organic Letters* **2017**, *19* (21), 5720-5723.
3. Mercer, S. M.; Andraos, J.; Jessop, P. G., Choosing the Greenest Synthesis: A Multivariate Metric Green Chemistry Exercise. *Journal of Chemical Education* **2012**, *89* (2), 215-220.
4. Manßen, M.; Deng, D.; Zheng, C. H. M.; DiPucchio, R. C.; Chen, D.; Schafer, L. L., Ureate Titanium Catalysts for Hydroaminoalkylation: Using Ligand Design to Increase Reactivity and Utility. *ACS Catalysis* **2021**, *11* (8), 4550-4560.
5. Daneshmand, P.; Roşca, S.-C.; Dalhoff, R.; Yin, K.; DiPucchio, R. C.; Ivanovich, R. A.; Polat, D. E.; Beauchemin, A. M.; Schafer, L. L., Cyclic Ureate Tantalum Catalyst for Preferential Hydroaminoalkylation with Aliphatic Amines: Mechanistic Insights into Substrate Controlled Reactivity. *J. Am. Chem. Soc.* **2020,** *142* (37), 15740-15750.
6. Hao, H.; Manßen, M.; Schafer, L. L., Tantalum Ureate Complexes for Photocatalytic Hydroaminoalkylation. *Chem. Sci*., SC-EDG-01-2023-000042.
7. Carter, W. P. L. UPDATED MAXIMUM INCREMENTAL REACTIVITY SCALE AND HYDROCARBON BIN REACTIVITIES FOR REGULATORY APPLICATIONS https://intra.engr.ucr.edu/~carter/SAPRC/MIR10.pdf.
8. Carter, W. P. L., Development of Ozone Reactivity Scales for Volatile Organic Compounds. *Air & Waste* **1994**, *44* (7), 881-899.
9. Allen, D. T.; Shonnard, D., *Green Engineering : Environmentally Conscious Design of Chemical Processes*. Upper Saddle River NJ: Prentice Hall PTR: 2002.
10. Heijungs, R.; Guinee, J.; Huppes, G.; Lankreijer, H. A.; Udo de Haes, A.; Wegner Sleewijk, A. M. M.; Ansems, P. G.; van Duin, R.; de Goode, H. P., *Environmental Life Cycle Assessment of Products*. CML, Leiden, The Netherlands: 1992.
11. Boethling, R. S.; Howard, P. H.; Meylan, W.; Stiteler, W.; Beauman, J.; Tirado, N., Group contribution method for predicting probability and rate of aerobic biodegradation. *Environmental Science & Technology* **1994**, *28* (3), 459-465.
12. Sheldon, R. A., Metrics of Green Chemistry and Sustainability: Past, Present, and Future. *ACS Sustainable Chemistry & Engineering* **2018**, *6* (1), 32-48.